CHAPTER 6

RESULTS OF GEOMETRIC MORPHOMETRIC ANALYSIS

Results of geometric morphometric analyses were broken into sections. Sections 6.1 and 6.2 focus on the results obtained from two perspectives (and their corresponding homologous landmarks) of changes to the distal and posterior humerus with the onset of age. The "EPI" perspective indicates the location of the angle of the medial epicondyle, photographed from the distal aspect when the humerus was placed with the posterior side up. The "OL" perspective shows the olecranon fossa and the bony structures surrounding it. Both perspectives were assigned a series of standardized landmarks from which to base the statistical queries.

Sections 6.3 and 6.4 focused on results of two perspectives (and their corresponding homologous landmarks) between males and females with the onset of age in the os coxae. The "SUB" perspective focused specifically on the morphological features of the subpubic concavity and the subpubic angle, while the "SCI" perspective elucidated the anatomy of the greater sciatic notch. Each subsequent section was delineated further into comparisons between age groups and populations, as seen in previous chapters.

6.1

Sexual dimorphism in the distal humerus: EPI perspective

Nineteen homologous landmarks were assigned to the distal humerus, as shown in Figure 3.26. In order to confirm that the distal and posterior humerus was sexually dimorphic, the first analyses focused on establishing the degree of dimorphism and the classification accuracies between females and males.

Consensus relative warp analysis performed with the statistical package tpsRelw required the comparison of at least four groups within a sample. Therefore, the sample was divided into four initial assemblages based on biological affiliation to observe the presence of sexual dimorphism in this anatomical perspective of the posterior humerus. This separation of the sample into "black" and "white" male and female populations was to determine whether significant differences occurred between the groups, and if sexual dimorphism was of a sufficient magnitude to influence the accuracy with which sex can be determined. The presence of sexual dimorphism in this skeletal element is illustrated in Figure 6.1.

As can be seen, a distinct sexually dimorphic component exists with the EPI perspective, as well as a population component. All females were viewed to group below the x-axis, while all males were viewed to group above the x-axis. In addition, the consensuses for white females and white males appear to the left of the y-axis, while the consensus for black females and black males appear to the right of the y-axis. Black males and black females appear relatively close to one another in this relative warp analysis, while white males and females are more separated.

6.1.1

Results from the EPI perspective between females and males

Figure 6.1 illustrates the differences between females and males of each biological group. Statistical analyses in the form of Goodall's F test from the IMP TwoGroup statistical package were performed to quantify the magnitude of differences between these groups. Goodall's F-test assesses inter-group shape disparity between each group, taking sample variance into account. Analyses were performed to observe the magnitude of these differences. Table 6.1 illustrates the statistically significant differences between all groups compared in Figure 6.1. Females and males of both ancestries were observed to be sexually dimorphic on a statistically significant level in the EPI perspective.

Table 6.1 confirmed the results visualized in Figure 6.1. Males and females appear to be sexually dimorphic on a significant level, as observed by their separation in the consensus relative warp grid. White males and females appear more sexually dimorphic than their black counterparts, based on the distance separating them on the relative warp grid, and the comparative Goodall's F-statistic (white females and males Goodall's F-statistic = 12.78, black females and males Goodall's F-statistic = 6.65).

A reference consensus thin-plate spline was created to view the mean shape of all the individuals in the sample for the EPI perspective. Figure 6.2 is a representation of the average shape of the all males and females exemplified by an exactly perpendicular grid. Figure 6.3 demonstrates the thin-plate spline for the deformation from the EPI perspective. The deformation grid exemplifies the areas of form breakdown from the perpendicular reference, in this case the female shape. The female shape would have appeared as a perfect perpendicular grid, and this figure now gives the degree of deformation of the males on this female reference grid. Figure 6.4 demonstrates the differences exhibited between females and males in thin-plate spline vector mode. Vector mode thus represents not only the differences in morphology, but also the direction and magnitude of that change. In Figure 6.4 the points (or circles) represent the first shape (female) while the arrows represent the direction of the male shape.

As seen in Figures 6.3 and 6.4, most discrepancy between females (the point of origin of the arrow in vector mode) and males (the end length of the arrow in vector mode) existed in the portion of the medial epicondyle. The "root" of the medial epicondyle (landmark six) is lower and more defined from landmark five, making the medial epicondyle sit more centrally within the trochlea, instead of positioning itself in a more distal location. The surface of the medial epicondyle was lower and more compact in males, with the most distal point (landmark ten) closer to the table on which the bone rested. The female medial epicondyle appeared more elevated

through landmarks 6 to 12. Differences could also be seen in the lateral portion of the posterior humerus, where the most lateral point in males (landmark 19) was located higher, and the medial margin of the lateral epicondyle (landmark 1) was located in a more elevated position, in contrast to the female lateral epicondylar ridge existing lower on the posterior humeral surface. Landmarks 16 and 17, which document the morphology of the anterior border of the capitulum and trochlea, appeared slightly constricted upwards in males.

The accuracy by which these differences in the distal humerus can assign specimens was assessed by means of a canonical variates analysis (CVA). A CVA can test the accuracy with which this particular aspect of the distal humerus can be categorized as female or male. Table 6.2 represents the accuracies obtained from this analysis.

Female specimens were correctly categorized 79% of the time, (129/163) while male specimens were 78% accurate in their morphology (143/ 184). The significance value obtained by the canonical variates analysis (148.185) was greater than the critical value of chi square distribution at the significance value of 0.05 with 30 degrees of freedom (43.773). Both males and females were categorized correctly a large percent of the time, thus showing that the differences observed during standard non-metric morphological assessment could also be observed when using geometric morphometrics, and are quantifiable.

6.1.2

Results from the EPI perspective: black females vs. males

Sexual dimorphism between black females and black males is shown in Figure 6.1, and the statistical significance between the sexes is quantified by Goodall's F-statistic in Table 6.1. Sexual dimorphism in this perspective was lower in black South Africans than in white South Africans. Females and males were thus

compared independently so as to visualize sexually dimorphic changes in the EPI perspective, and to observe any differences in this specific sample.

Figure 6.5 demonstrates the thin-plate spline in deformation mode, which indicates the location on the EPI perspective where males deviate from the female reference grid. A warped or deformed portion of the grid designates morphological difference. Figure 6.6 is the thin-plate spline in vector mode, which illustrates the differences between black females and black males from the EPI perspective. Vector mode represents the direction and magnitude of change between the sexes in the sample. In Figure 6.6 the points (or circles) represent the first shape represented (black females) while the arrows represent the direction of the black male shape.

As seen in Figure 6.5, most discrepancy between black females and black males occurred along the lateral margin, which "tilted" the graph downwards on the left-hand (lateral) margin. Deformation was also observed along the points around the medial epicondyle. In vector mode as seen from Figure 6.6, females (the point of origin of the arrow in vector mode) and black males (the end length of the arrow in vector mode) differ in that the medial ridge of the lateral epicondyle (landmark 1) sits lower, or more towards the anterior, in males. This change of anteriorly migrating landmarks repeats with landmarks 18 and 19. In addition, landmark 15, the inferior edge of the trochlea, was seen to be higher in males, giving the inferior "spool" view of the humerus a less-constricted shape. Landmarks along the anterior surface of the medial epicondyle (landmarks 10 through 14) were observed to be higher in males than females. From this perspective, the medial epicondyle appears thinner in males than females. Because if this, the medial epicondyle in males may appear more angled away from the table with the position of landmarks 10 through 14; this angled aspect of the medial epicondyle is considered a "female" characteristic.

The accuracy by which these differences in the distal humerus can assign black South African specimens was assessed by means of a canonical variates analysis (CVA). A CVA can test the accuracy with which this particular aspect of the

distal humerus can be categorized as female or male. Table 6.3 represents the accuracies obtained from this analysis.

Black female specimens were correctly categorized 83% of the time, (83/ 100) while male specimens were 85% accurate (85/ 108). The significance value obtained by the canonical variates analysis (110.017) was greater than the critical value of chi square distribution at the significance value of 0.05 with 30 degrees of freedom (43.773). The classification accuracy was high for both black females and black males, thus showing that the sexual dimorphism in this population was quantifiable when using geometric morphometrics.

6.1.3

Results from the EPI perspective: white females vs. males

Sexual dimorphism between white females and white males was seen in Figure 6.1, as white females and white males appeared in different quadrants of a four-quadrant grid. The subsequent statistical significance between the sexes was quantified by Goodall's F-statistic in Table 6.1. Using this perspective, sexual dimorphism was evident for this group. Females and males were thus compared in this population independently so as to visualize these sexually dimorphic changes in the EPI perspective, and to observe any differences between the white and black samples.

Figure 6.7 demonstrates the thin-plate spline in deformation mode between females and males of the white group, which demonstrates the deviation males have from a perfect perpendicular grid (the female mean). Deformation in Figure 6.7 was seen primarily in the homologous landmarks placed around the medial epicondyle. Figure 6.8 subsequently shows the thin-plate spline in vector mode, which illustrates the magnitude and direction of differences between white females and white males from the EPI perspective. In Figure 6.7 the points (or circles) represent the first

shape represented (white female) while the arrows represent the direction of the white male shape.

As seen in Figure 6.8, females exhibited a markedly "raised" or angled medial epicondyle (considered classic "female" morphology), while male landmarks placed around this feature (landmarks 7 through 12) appeared lower and more towards the anterior surface of the bone. This would account for a more parallel angle to the medial epicondyle, which was considered a classic "male" profile. In addition, the landmarks placed on the lateral surface of the distal humerus (landmarks 18 and 19) were farther posteriorly on the male perspective than on the female perspective. These differences were similar to those seen in black South Africans in that the majority of the variation between males and females was observed through the surface of the medial epicondyle.

The accuracy by which these differences in the distal humerus can assign white specimens was assessed by means of a canonical variates (CVA) analysis. A CVA tests the accuracy with which this particular aspect of the distal humerus can be categorized as female or male. Table 6.4 represents the accuracies obtained from this analysis.

Female specimens were correctly categorized 91% of the time, (57/ 63) when compared to white males. White male specimens were classified at a 90% accuracy rate (68/ 76). The significance value obtained by the canonical variates analysis (107.188) was greater than the critical value of chi square distribution at the significance value of 0.05 with 30 degrees of freedom (43.773). The classification accuracy was high for both white females and white males, thus showing that the sexual dimorphism in this population was quantifiable when using geometric morphometrics.

Each biological affiliation, as well as the combined data of all females and all males, exhibited marked sexual dimorphism from the EPI perspective. Thus sexual dimorphism could be quantified, and correct classification of males and females was

sample used.

6.1.4

Sexual dimorphism and the onset of age: EPI perspective

Analyses were then performed in order to discern if characteristics from this perspective changed with the onset of age. Thus, each biological group and both sexes were further categorized as "young" (50 years of age or younger) and "old" (over 50 years of age). This provided an amalgamation of eight groups: young black females, young white females, old black females, old white females, young black males, young white males, old black males and old white males. The differences between males and females from each age group were subsequently examined.

A consensus relative warp analysis on all eight possible groups for the EPI perspective was performed to visualize the groupings between each combination of the sample (Figure 6.9). All eight permutations (1. young black female, 2. young white female, 3. old black female, 4. old white female, 5. young black male, 6. young white male, 7. old black male, 8. old white male) separate to a certain extent and cluster to a certain degree. Thus it is clear that there are differences between males and females, but population affinity and variations in age may also play roles in the separation of these groups.

Young and old groups appear commingled together, while those grouped in the black and white populations appear to cluster separately on the left and right side of the medial Y-axis, respectively. Females of each population clustered together (above the horizontal axis), and males of each population and age were observed to cluster together (mostly below the horizontal axis). Figure 6.9 also illustrates that young individuals of each biological affinity are quite separated from each other, while the old individuals of each biological affinity appear to "migrate" towards each other and become more similar.

6.1.5

Sexual dimorphism and the onset of age: black females and males

Evidence represented in Figure 6.9 shows that differences exist between black males and females, and that morphology of the posterior humerus from the EPI perspective appears to differ between young and old individuals. First, consensus thin-plate splines in vector mode were created for black females and black males independently to observe the differences between young and old consensus shapes. Figure 6.10 is the thin-plate spline in vector mode that exemplifies the changes females underwent with the onset of age.

As seen in Figure 6.10, changes from the young black female shape to the old black female shape took place primarily in the lateral and posterior surfaces of the perspective. Vector mode illustrates this expansion of the lateral and posterior surface. Landmarks 15 and 16 become lower along the border of the trochlea (which is medial) while landmarks 1, 2, 18 and 19 (all situated laterally) expand upwards, creating a thicker lateral portion. Changes in the medial epicondyle and its angle in the black female with age were minimal.

The changes that occur with age in black males can be seen in Figure 6.11. This graph shows the vector mode for black males as it transforms from "young" morphology to "old" morphology. Differences between young black males and old black males existed along the lateral and medial edges. These changes with the black male EPI perspective with age appeared more marked than in their female counterparts.

When observing the vector mode, several morphological differences are apparent. Landmark 1 appeared to rise higher, making the medial ridge of the lateral epicondyle more apparent. Landmark 14 was viewed lower or more anteriorly in old males, making the medial epicondyle take on a thicker appearance where it joins the trochlea. Landmark 15 also appeared lower (or more anteriorly) while landmark 17

rose upwards; the combination of this result may indicate more constriction within the area between the capitulum and the trochlea. Finally, landmarks 18 and 19 migrated towards the posterior, placing the tip of the lateral epicondyle and the lateral margin of the capitulum in a more posterior position.

Through viewing the direction and magnitude of change in thin-plate spline vector mode analyses, changes in black males and females with the onset of age were observable (Figures 6.10 and 6.11). In addition, Goodall's F-statistic comparing the young black sample (young black females vs. young black males) and the old black sample (old black females vs. old black males) was significant for both groups, but as seen in Table 6.5, the strength of the statistical significance decreased with the old sample (Goodall's F-statistic for the young sample = 5.50, df = 30, p = 0.000<0.05; Goodall's F-statistic for the old sample = 3.72, df = 30, 0.000<0.05). Because obvious changes were seen with age, the classification accuracies of both young and old individuals were calculated as a means to test whether sex could still be correctly assigned to the aged sample.

Table 6.6 illustrates the classification accuracy between males and females of both age groups. As can be seen in this table, young black individuals were classified at a high rate of accuracy when compared to each other (94% accurate for young black females, 89% accurate for young black males). The correct assignment of sex actually increased with the onset of age for old black females and old black males (96% and 94%, respectively). Both sets of changes were deemed statistically significant. This assessment of changes occurring with age may indicate that as the black population gets older, the classic "male" and "female" morphology of the inferior humerus and the angle of the medial epicondyle became more sexually dimorphic, and thus a higher percentage of individuals may be correctly classified. Changes with age to the distal humerus in the EPI perspective did not influence the classification accuracy for black South Africans. This trait is consistent in sorting between males and females regardless of age.

6.1.6

Sexual dimorphism and the onset of age: white females and males

In contrast to that observed in black South Africans, evidence represented in Figure 6.9 showed that differences existed between white males and females for the morphology of the posterior humerus from the EPI perspective. Consensus thin-plate splines in vector mode were created for white females and white males to observe the differences between young and old consensus shapes. Figure 6.12 is the thin-plate spline in vector mode that exemplified the changes white females underwent with the onset of age.

In vector mode, the landmarks in the region of the medial epicondyle (landmarks 7 through 14) appeared to increase in elevation and angle both posteriorly and medially from the young white female morphology (circles) to the old white female morphology (arrows). This result would create the appearance of a more slanting or "raised" medial epicondyle angle. Based on the fact that a posteriorly slanting medial epicondyle is considered a distinctly female characteristic, this may produce more explicit sexual dimorphism in old white females from the EPI perspective. Thus, old white females will take on a more classic "female" appearance.

In addition, the lateral surfaces of the medial epicondyle appeared to migrate towards the anterior surface. Landmarks 1, 2, 3, 16, 17, 18 and 19 shifted anteriorly from young white females to old white females, which may have created a less-constricted anterior capitulum spool and a thinner lateral epicondyle.

Young white males and old white males did exhibit small morphological differences, as seen in the relative warp analysis in Figure 6.9. To visualize these differences, thin-plate splines were created in vector mode to observe the location and direction of variation between the young white male EPI perspective, and the old white male EPI perspective. The changes that occur with age in white males can be

seen in Figure 6.13. This graph shows the vector mode for white males as it transforms from "young" morphology to "old" morphology.

As seen in Figure 6.13, differences between young white males and old white males existed along the lateral and medial edges. The vector arrows indicated directional change, where the posterior margin of the lateral epicondyle descended (landmark 1), as did landmarks three and four placed within the curvature of the distal posterior humeral surface. The posterior "root" of the medial epicondyle, represented by landmark six, migrated closer towards landmark five. This result would place the medial epicondyle more posteriorly within the profile of the trochlea, which is a more distinctly "female" characteristic.

Changes in white males and females with the onset of age were observable by viewing the direction and magnitude of change in thin-plate spline vector mode analyses (Figures 6.12 and 6.13). Visible changes in the white female EPI perspective were apparent; white female morphology appeared to diverge in numerous locations. In addition, Goodall's F-statistic comparing the young white sample (young white females vs. young white males) and the old sample (old white females vs. old white males) was significant for both groups, but as seen in Table 6.7, the significance in the statistic was not as considerable between young males and females (Goodall's F-statistic for the young sample = 4.44, df = 30, p = 0.014<0.05; Goodall's F-statistic for the old sample = 8.80, df = 30, 0.000<0.05). Because obvious changes were seen with age, the classification accuracies of both young and old individuals were calculated to determine if this accuracy rate decreased with the aging morphology of the white population.

Table 6.8 illustrates the classification accuracy between males and females of both age groups. As can be seen in this table, canonical variates analysis from the IMP statistical package could not correctly distinguish young white females from young white males with the EPI perspective; no statistics were generated when the analysis was performed. This indicated that the morphology of the EPI perspective

with these two groups compared was virtually the same. The sample size of the young population may also have played a role in the inability to perform statistical analysis. Old white females and males, however, were sorted successfully when compared to each other. Old white females were classified correctly 92% of the time when compared to their old male counterparts. The old male sample was classified at a rate of 85% accuracy. This assessment of changes occurring with age may indicate that as the white population gets older, the classic "male" and "female" morphology of the inferior humerus and the angle of the medial epicondyle become more sexually dimorphic, and thus a higher percentage of individuals may be correctly classified. Sexual dimorphism appeared to increase; with the females, in particular, becoming more "female" in their morphology, and the males acquiring a slightly more "male" morphology. Changes with age to the distal humerus in the EPI perspective did influence the classification accuracy for this biological group. The younger group appeared to exhibit more ambiguous or variable morphology from the EPI view than the older group.

6.2

Sexual dimorphism in the distal humerus: OL perspective

Fifteen homologous landmarks were assigned to the posterior humerus, as shown in Figure 3.27. The OL perspective quantified characteristics of the distal humerus that included the olecranon fossa shape and trochlear extension through landmark data analysis. In order to confirm that the posterior humerus was sexually dimorphic, the first analyses focused on establishing the degree of dimorphism and the classification accuracies between females and males. Consensus relative warp analysis performed with the statistical package tpsRelw required the comparison of a

minimum of four groups within a sample. Therefore, the sample was divided into four initial assemblages based on biological affiliation to observe the presence of sexual dimorphism in this anatomical perspective of the posterior humerus. This separation of the sample into "black" and "white" male and female populations was to determine whether significant differences occurred between the groups, and if sexual dimorphism was of a sufficient magnitude to influence the accuracy with which sex can be determined. The presence of sexual dimorphism in this skeletal element is illustrated in Figure 6.14.

As can be seen, a distinct sexually dimorphic component existed with the OL perspective, as well as a population component. All females were viewed to group below the x-axis, while all males were viewed to group above the x-axis. In addition, the consensuses for white females and white males appear to the left of the y-axis, while the consensus for black females and black males appear to the right of the y-axis. This initially indicated that the OL perspective and its quantified morphology might be distinct between males and females as well as between black and white South Africans.

6.2.1

Results from the OL perspective between females and males

Figure 6.14 illustrates the differences between females and males of each group, but does not indicate a statistical significance between those present in the assemblage. Statistical analyses in the form of Goodall's F test from the IMP TwoGroup statistical package was performed to quantify the magnitude of differences between the above four groups. Goodall's F-test assesses inter-group shape disparity between groups, taking sample variance into account. Analyses were performed to observe the magnitude of these differences. Table 6.9 illustrates the statistically significant differences between all groups compared in Figure 6.14.

Females and males of both ancestral groups were observed to be sexually dimorphic on a statistically significant level with the OL perspective.

Table 6.9 confirmed the results visualized in Figure 6.14. Males and females appear to be sexually dimorphic on a significant level, as observed by their separation in the consensus relative warp grid and by their significant Goodall's F-statistic. All permutations seen in Table 6.9 were significantly different enough to deem the OL perspective and the shape of the olecranon fossa sexually dimorphic.

A reference consensus thin-plate spline was created to view the mean shape of all the individuals in the sample for the OL perspective. Figure 6.15 is a representation of the average shape of the all males and females exemplified by an exactly perpendicular grid. Figure 6.16 demonstrates the thin-plate spline for the deformation from the OL perspective. The deformation grid exemplifies the areas of form breakdown from the perpendicular reference, in this case the female shape. The female shape would have appeared as a perfect perpendicular grid, and this figure now gives the degree and deformation of the males on this female/ reference grid. Figure 6.17 demonstrates the differences exhibited between females and males in thin-plate spline vector mode. Vector mode thus represents not only the differences in morphology, but also the direction and magnitude of that change. In Figure 6.17 the points (or circles) represent the first shape represented (females) while the arrows represent the direction of the male shape.

As seen in Figures 6.16 and 6.17, discrepancy between females (the point of origin of the arrow in vector mode) and males (the end length of the arrow in vector mode) existed in the olecranon fossa shape and the distal boundary of this view of the humerus. Females appeared to have a lower (more posteriorly placed) superior margin of the olecranon fossa. Landmark five, the point that makes the olecranon fossa decidedly oval (in females) or triangular (in males) is placed higher along the medial shaft of the bone with males. Subsequently, this would create a more triangular shape in the male olecranon fossa. This finding corresponds to the visual

characteristic in which males exhibited triangular olecranon fossa shapes (thus exhibiting a higher superior olecranon fossa margin, indicated by landmark five) and females have an oval olecranon fossa shape (exhibited by a lower superior olecranon fossa margin). Landmark 1 is in direct correlation with this observation, because it is based on the most-superior point on the olecranon fossa. As Figure 6.17 has shown, it also appears higher than the female adaptation of landmark 1. In addition, the medial margin of the olecranon fossa was located more posteriorly than females, indicated by landmark four. The most lateral point of the lateral epicondyle (landmark 11) is also higher in males than in females, while landmark 12 (denoting the most medial point of the medial epicondyle) appeared farther distally in males than females. Landmarks 13, 14 and 15 indicate the inferior border of the distal humerus. The edge of the posterior capitulum (landmark 13) was higher in males than females. This result, coupled with the extension and projection of the edge of the posterior trochlea (landmark fifteen) created a more "extended" trochlea past the margin of the capitulum, a feature that is considered to be distinctly "male". It appeared as if this feature (trochlear extension) might be successfully quantified as sexually dimorphic in addition to the shape of the olecranon fossa.

The accuracy by which these differences in the distal humerus can assign a specimen was assessed by means of a canonical variates analysis (CVA). Table 6.10 represents the accuracies obtained from this analysis.

Female specimens were correctly categorized 83% of the time (135/163) and male specimens 84% (156/ 185). As shown by the chi square value of 211.344 (significant at $p<0.05$) the OL perspective, which included a quantitative observation of the olecranon fossa shape as well as the extension of the trochlea, was sexually dimorphic on a statistically significant level. Males and females could be classified accurately 83% to 84% of the time.

6.2.2

Results from the OL perspective: black females vs. males

Sexual dimorphism between black females and black males was shown in Figure 6.14, and the statistical significance between the sexes was quantified by Goodall's F-statistic in Table 6.9. Sexual dimorphism in this perspective was higher in black South Africans than in white South Africans. Females and males were thus compared in this population independently so as to visualize these sexually dimorphic changes in the OL with sex and the onset of age.

Figure 6.18 demonstrates the thin-plate spline in deformation mode, which indicates the location on the OL perspective where females and males deviate from each other. A warped or deformed portion of the grid designates morphological difference. Figure 6.19 is the thin-plate spline in vector mode, which illustrates the differences between black females and black males from the OL perspective. In Figure 6.19 the points (or circles) represent the first shape represented (black female) while the arrows represent the direction of the black male shape.

As seen in Figure 6.18, most discrepancy between black females and black males occurred along the peripheral margins, which "tilted" the graph downwards on the right-hand (medial) margin. In vector mode as seen from Figure 6.19, black females (the point of origin of the arrow in vector mode) and black males (the end length of the arrow in vector mode) differ in that both lateral landmarks 1 and 11 appeared superiorly in males. The medial corresponding landmark that indicated the tip of the medial epicondyle (landmark 12) subsequently was viewed to be more inferior in males. Additional differences between black females and black males were exhibited along the inferior border of the humerus. The distal margin of the capitulum appeared higher in males (landmark 13). In addition, the distal margin of the trochlea appeared lower and more extended in males (landmark 15). This would create the visual characteristic of a more inferiorly projecting trochlea past the margin

of the capitulum from this perspective. This result is analogous to the total population thin-plate spline between females and males (Figure 6.17). Again, this extension of the trochlear margin was considered a distinctly male trait in non-metric morphology.

The accuracy by which these differences in the distal humerus can assign black specimens was assessed by means of a canonical variates (CVA) analysis (Table 6.11). Black female specimens were correctly categorized 82% of the time, (82/ 100) while male specimens were 81% accurate (89/ 110). The value obtained by the canonical variates analysis (123.551) was significant at $p < 0.05$. The classification accuracy was high enough such that sexual dimorphism fro the OL perspective is quantifiable in black females and males

6.2.3

Results from the OL perspective: white females vs. males

Sexual dimorphism between white females and white males was seen in Figure 6.14, as these groups appeared in different quadrants of a four-quadrant grid. The subsequent statistical significance between the sexes was quantified by Goodall's F-statistic in Table 6.9. Females and males were thus compared independently so as to visualize differences between the sexes and with the onset of age.

Figure 6.20 demonstrates the thin-plate spline in deformation mode between females and males, which demonstrates the deviation males have from a perfect perpendicular grid (the female mean). Deformation in Figure 6.20 was seen primarily in the homologous landmarks placed around the periphery of the distal humerus. Figure 6.21 subsequently shows the thin-plate spline in vector mode. In Figure 6.21 the points (or circles) represent the first shape represented (white females) while the arrows represent the direction of the white male shape.

As seen in Figure 6.21, those landmarks that denote the superior margin of the olecranon fossa (corresponding landmarks 1, 2, and 5) appear higher in the male

than the female humerus. This indicates the olecranon fossa projected farther up the medial shaft of the humerus in males, creating a more triangular shape in that region of the fossa. In addition, the projection of the inferior trochlea (landmark 15) appeared greater in males than in females. Landmark 15 appeared to project medially as well, causing the extension past the inferior margin of the capitulum (landmark 13) to be more pronounced in males. In all, the differences around the periphery of the trochlea and capitulum seemed to be more pronounced than differences seen in the olecranon fossa.

The accuracy by which these differences in the distal humerus can assign sex was assessed by means of a canonical variates (CVA) analysis. Table 6.12 represents the accuracies obtained from this analysis. Females were correctly categorized 87% of the time, (55/ 63) and males 88% (66/ 75). This was statistically significant at $p<0.05$. Therefore, this trait is sexually dimorphic and can be quantifiable when using geometric morphometrics in the OL perspective.

6.2.4

Sexual dimorphism and the onset of age: OL perspective

A quantifiable difference between males and females in both populations was observed when applying geometric morphometrics to the OL perspective, a view that exemplifies the olecranon fossa shape and trochlear extension in the posterior and distal humerus. This combination of these two characteristics was thus shown to be sexually dimorphic on a statistically significant level. Analyses were then performed in order to discern if characteristics from this perspective changed with the onset of age. Thus, each biological affiliation and both sexes were further categorized as "young" (50 years of age or younger) and "old" (over 50 years of age). This provided an amalgamation of eight groups: young black females, young white females, old black females, old white females, young black males, young white males, old black

males and old white males. The differences between males and females from each age group were subsequently examined.

A consensus relative warp analysis on all eight possible groups for the OL perspective was performed to visualize the groupings between each combination of the sample (Figure 6.22). All eight permutations (1. young black female, 2. young white female, 3. old black female, 4. old white female, 5. young black male, 6. young white male, 7. old black male, 8. old white male) separate into distinctive groupings or "clusters". Females of each biological affiliation clustered together, as did males of each affiliation. Females were observed below the margin of the x-axis, while males were above the x-axis. This indicated that the quantification of the OL perspective was sexually dimorphic. Young and old groups appeared to cluster together, which indicated that this characteristic changed little with age. Those grouped in the black and white groups appear to cluster separately on the right and left side of the medial Y-axis, respectively.

6.2.5

Sexual dimorphism and the onset of age: black females and males

Evidence represented in Figures 6.14 and 6.22 shows that differences exist between black males and females, and that morphology of the posterior humerus from the OL perspective varied little between the age groupings of "young" and "old". First, consensus thin-plate splines in vector mode were created for black females and males independently to observe the differences between young and old consensus shapes.

Figure 6.23 is the thin-plate spline in vector mode that exemplifies the changes black females underwent with the onset of age. The lateral and medial ridges of the humerus above both epicondyles migrated inferiorly and superiorly (landmark 1 and 2, respectively). The lateral and medial edges of each epicondyle migrated inferiorly and superiorly (landmark 11 and 12, respectively). Landmark 13,

the inferior margin of the capitulum, extended farther inferiorly while the inferior margin of the trochlea (landmark 15) contracted farther superiorly in old black females. These two changes between young black females and old black females would possibly cause a loss of trochlear extension in this portion of the humerus. A lack of trochlear extension (where the inferior edge of the capitulum and the inferior edge of the trochlea were more equal) was considered a distinctly "female" characteristic.

Each group of black females was different based on the separation from the relative warp analysis grid. This separation did not appear considerable, based on the fact that each clustered together in the lower right-hand portion of a four-quadrant grid. The subsequent canonical variates analysis, however, confirmed that the difference between young and old black females was great enough to quantify and categorize each with a high degree of accuracy.

The changes that occur with age in black males can be seen in Figure 6.24. This graph shows the vector mode for black males as it transforms from "young" morphology to "old" morphology. As seen in Figure 6.24, minimal changes were observed. The most lateral point of the olecranon fossa (landmark 3) travelled to a more superior position in old black males, while the lateral edge of the lateral epicondyle was seen to once again move superiorly as the medial edge of the medial epicondyle (landmark 12) positioned itself more inferiorly. Finally, the inferior edge of the trochlea (landmark 15) was observed to extend more inferiorly, and migrate slightly medially as well. These differences did appear subtle.

Changes in black males and females with the onset of age were observable by viewing the direction and magnitude of change in thin-plate spline vector mode analyses (Figures 6.23 and 6.24). In addition, Goodall's F-statistic comparing the young (young black females vs. young black males) and the old (old black females vs. old black males) was statistically significant. As seen in Table 6.13, the significance in the statistic decreased with the old sample (Goodall's F-statistic for

the young sample = 5.80, df = 22, p = 0.000<0.05; Goodall's F-statistic for the old sample = 2.45, df = 22, 0.000<0.05). Because obvious changes were seen with age, the classification accuracies were calculated and compared so as to observe a change, if any, to the assignment of sex with the onset of age.

Table 6.14 illustrates the classification accuracy between males and females of both age groups. As can be seen in this table, young black individuals were classified at a high rate of accuracy when compared to each other (84% accurate for young black females, 95% for young black males). The high classification rate indicates that males, when grouped in a young age category, exhibit marked male morphology that was easily quantifiable and discernable from the female shape.

Classification accuracy decreased for males with the onset of age (95% to 85%). This may indicate that as the black population gets older, the classic "male" and "female" morphology of distal humerus, including features such as the olecranon fossa shape, become less sexually dimorphic, and thus the ability to correctly assign a specimen to male or female declined.

6.2.6

Sexual dimorphism and the onset of age: white females and males

Evidence represented in Figures 6.14 and 6.22 showed that differences existed between white males and females, and that morphology of the distal humerus from the OL perspective appeared to not differ greatly between young and old individuals. Refer to Figure 6.22 for a summary of the clustering exhibited by all eight permutations in the OL perspective. Consensus thin-plate splines in vector mode were created for white females and males to observe the differences between young and old consensus shapes.

Figure 6.25 is the thin-plate spline in vector mode that exemplified the differences between young and old white females. The thin-plate spline in vector mode showed that little movement of homologous landmarks took place. The lateral

margin of the lateral epicondyle (landmark 11) migrated more superiorly between white females in the "young" and "old" groups. Landmark 13, the inferior margin of the capitulum, also migrated more superiorly in old white females, indicating an increase in trochlear extension on the medial side. This would provide a less "female" profile of the capitulum compared to the trochlea, which should be more equal in females. Landmark 2, the point placed upon the medial epicondylar ridge, moved inferiorly with age to a position lower than that of the young white female. In general, the morphological features of olecranon fossa shape and trochlear extension appeared to stay largely the same with the onset of age in the white female humerus.

Young white males and old white males did exhibit small morphological differences, as seen in the relative warp analysis in Figure 6.22. To visualize these differences, a thin-plate spline was created in vector mode to observe the location and direction of variation between the young and old in the OL perspective (Figure 6.26). Figure 6.26 indicated a lack of any variation with the absence of arrows indicating the direction of variation.

Small changes in white males and females with the onset of age were observable by viewing the direction and magnitude of change in thin-plate spline vector mode analyses (Figures 6.25 and 6.26). Goodall's F-statistic comparing the young white sample (young white females vs. young white males) and the old (old white females vs. old white males) were statistically significant for both groups, but as seen in Table 6.15, the significance in the statistic appeared to be greater with the old sample (Goodall's F-statistic for the young sample = 1.79, df = 22, p = 0.022<0.05; Goodall's F-statistic for the old sample = 3.32, df = 22, 0.000<0.05). Because the changes in the white population were very subtle with the OL perspective, the classification accuracies were calculated and compared so as to observe a change, if any, to the assignment of sex with the onset of age.

Table 6.16 illustrates the classification accuracy between males and females of both age groups. As can be seen in this table, young individuals were classified at a 92-100% rate of accuracy when compared to each other (92% accurate for young white females, 100% accurate for young white males). This shows females and males within this small sub-group of the white population exhibit enough divergent morphology to be categorized correctly the majority of the time. This classification accuracy was unusually high for any characteristic categorizing the differences between males and females. The small sample size for young white individuals (13 for females, 23 for males) may have played a role in the canonical variates analysis results being uncommonly accurate.

Classification accuracy decreased slightly with the onset of age in the white sample, however. Old white females and males were each classified correctly 90% of the time. This assessment of changes occurring with age may indicate that as the white population gets older, the classic "male" and "female" morphology of the inferior humerus and the angle of the medial epicondyle stayed relatively static in its sexual dimorphism. Females exhibited quantifiable "female" characteristics in the OL perspective, and these characteristics did not change with the onset of age, allowing for old females to be categorized correctly even when older individuals were assessed. Males exhibited the same absence of change with the onset of age. Morphological modification with age to the distal humerus in the OL perspective did not adversely influence the classification accuracy for this sample.

Although females and males from different samples exhibited variation in their classification accuracy, the OL perspective remained a good indicator of sex, when the shape of the olecranon fossa and the extension of the trochlea were quantified. Thus the OL perspective can bee seen as a sexually dimorphic feature that changes only subtly with the onset of age.

6.3

Sexual dimorphism in the pelvis: SUB perspective

Twenty-eight homologous landmarks were assigned to the subpubic portion of the pelvic bone as shown in Figure 3.28. The SUB perspective quantified characteristics of the subpubic concavity and subpubic angle through landmark data analysis. This view also included landmarks around the margin of the obturator foramen. The obturator foramen landmarks were included only to provide distinctive points of extrapolation for homologous landmarks placed around the periphery of the pubis and ischium, and its influence in the categorization of sex appeared minimal in this capacity. Even though the obturator foramen was not intended to provide results or influence the morphology of the subpubic region of the pelvis, changes in its morphology were noted when they were observed.

In order to confirm that the pubic region of the pelvis was sexually dimorphic, the first analyses focused on establishing the degree of dimorphism and the classification accuracies between females and males. Consensus relative warp analysis performed with the statistical package tpsRelw required the comparison of a minimum of four groups within a sample. Therefore, the sample was divided into four initial assemblages.

As can be seen in Figure 6.27, a distinct sexually dimorphic component existed with the SUB perspective, as well as a smaller population component. All females were viewed to group to the right of the y-axis, while all males were viewed to the left of the y-axis. Females, although in different quadrants of the four-quadrant graph, appeared relatively close together. Males, although on the same side of the y-axis, and approximately the same distance apart from the females, appeared to diverge dramatically from each other, indicating a difference in morphology between groups. The consensuses for white females and white males appeared above the x-axis, while the consensus for black females and black males appeared below the x-

axis. This initially indicated that the SUB perspective and its quantified morphology might be distinct between males and females. In addition, biological affiliations appeared to separate to a lesser degree into different morphological forms as well.

6.3.1 Results from the SUB perspective between females and males

Figure 6.27 illustrates the differences between females and males of each group, but does not indicate a statistical significance between those present in the assemblage. Statistical analyses in the form of Goodall's F test from the IMP TwoGroup statistical package were performed to observe the magnitude of these differences. Table 6.17 illustrates the statistically significant differences between all groups compared in Figure 6.27. Females and males, regardless of biological affiliation, were observed to be sexually dimorphic on a statistically significant level with the SUB perspective.

Males and females, regardless of their population, appeared distinctly apart from each other. Females of both population groups appeared closer together in consensus morphology than their male counterparts; it appeared as if black males and white males differed considerably in their anatomical features when the consensus relative warp grid was assessed. In addition, black females and males might be more sexually dimorphic than their white counterparts, based on the comparative Goodall's F-statistic (white females and males Goodall's F-statistic = 30.09, black females and males Goodall's F-statistic = 36.59). Both, however, were significantly different enough to deem the SUB perspective and the shape of the subpubic angle sexually dimorphic.

A reference consensus thin-plate spline was created to view the mean shape of all the individuals in the sample for the SUB perspective. Figure 6.28 is a representation of the average shape of males and females exemplified by an exactly perpendicular grid. Figure 6.29 demonstrates the thin-plate spline for deformation

from the SUB perspective. The deformation grid exemplifies the areas of form breakdown from the perpendicular reference, in this case the female shape. The female shape would have appeared as a perfect perpendicular grid, and this figure now gives the degree and deformation of the males on this female/ reference grid. The deformation grid exhibited a large amount of warping and collapse along all borders where homologous landmarks were placed. Figure 6.30 demonstrates the differences between females and males in thin-plate spline vector mode. Vector mode thus represents not only the differences in morphology, but also the direction and magnitude of that change. In Figure 6.30 the points (or circles) represent the first shape represented (female) while the arrows represent the direction of the male shape.

As seen in Figures 6.29 and 6.30, discrepancy between females (the point of origin of the arrow in vector mode) and males (the end length of the arrow in vector mode) existed in the length of the pubis (landmarks 14-18), the width of the ischium (landmarks 21, 22, 24, 27 and 28), the shape of the subpubic concavity (landmarks 19, 23, 25 and 26) and the obturator foramen shape (landmarks 1-13). The vector mode thin-plate spline illustrated numerous differences between males and females in the pelvic morphology of the subpubic angle and subpubic concavity. Based on landmarks 2, 5, 10 and 11 within the obturator foramen, it appears that the male obturator foramen (the end of the arrow boundaries) was wider through the inferior and dorsal margins than females (points). Landmarks 14 through 20 (demarcating the pubis bone and the vertical pubic symphysis) illustrated that this portion of the pelvis was much shorter in males than females. Male points in this region were seen to exist farther towards the acetabulum. In addition, landmarks 21, 23, 25 and 26 along the subpubic concavity were shorter and more medially inclined in the male than the female pelvis. This would create a thicker ischium and a narrow subpubic concavity without much extension or angling as it extended towards the ischium.

Finally, landmarks 22, 24, 27 and 28 demonstrated that the male ischium throughout this region was wider and thicker than that of females.

The accuracy by which these differences in the pelvis can assign a specimen was assessed by means of a canonical variates (CVA) analysis. Table 6.18 represents the accuracies obtained from this analysis.

Both females and males were correctly categorized 94% of the time (135/143 females; 165/ 175 males). The chi square value obtained by the canonical variates analysis was significant at the 0.05 level, which indicated that the SUB perspective, which included a quantitative observation of the subpubic angle and the subpubic concavity, was sexually dimorphic on a statistically significant level.

6.3.2

Results from the SUB perspective: black females vs. males

Sexual dimorphism between black females and males was initially shown in Figure 6.27, and the statistical significance between the sexes was quantified by Goodall's F-statistic in Table 6.17. Sexual dimorphism in this perspective appeared more statistically significant in this sample than in the white sample. Sex was compared independently so as to visualize sexually dimorphic differences in the SUB perspective and to observe any changes.

Figure 6.31 demonstrates the thin-plate spline in deformation mode, which indicates the location on the SUB perspective where females and males deviate from each other. A warped or deformed portion of the grid designates morphological difference. Figure 6.32 is the thin-plate spline in vector mode, which illustrates the differences between black females and males from the SUB perspective. As in previous graphs, the points (or circles) represent the first shape represented (black female) while the arrows represent the direction of the black male shape.

As seen in Figure 6.31, the most deformation between females and males occurred along the peripheral margin of the pubic bone and directly below the inferior

margin of the pubic symphysis, the location where the subpubic concavity is visualized. These differences were similar to what was observed in the combined male and female graph, but occurring to a lesser degree. These deformations between females (as the reference) and males (as the deformation) "tilted" the graph downwards on the right-hand (medial) margin. In vector mode as seen from Figure 6.32, females (the point of origin of the arrow in vector mode) and males (the end length of the arrow in vector mode) differ in that the landmarks assigned to the superior border of the pubis (landmarks 14 through 18) are positioned more superiorly in the male than in the female sample. This would visually give the pubis a thicker profile in males than in females. The landmarks which designated the subpubic angle and subpubic concavity (landmarks 19, 21, 23, 25 and 26) appear elongated and extended in the black females. In contrast, these same points in the black male sample appear closer to the acetabulum, truncating this segment of bone into appearing thicker, less angled, and contributed to a narrower subpubic angle. The obturator foramen showed little difference between females and males. Landmarks 1, 7, and 13 were positioned more superiorly in black males, giving the foramen a wider appearance through this portion of the feature. Other homologous landmarks around the border of the obturator foramen did not exhibit differences between males and females of this sample.

The accuracy by which these differences in the SUB perspective of the pelvis can assign black specimens was assessed by means of a canonical variates (CVA) analysis (Table 6.19). Black females were correctly categorized 96% of the time, (82/ 85) while males were 98% accurate (101/ 103). This is significant at $p<0.05$. The classification accuracy was high enough for both females and males to show that the sexual dimorphism in this population was quantifiable when using geometric morphometrics from the SUB perspective.

6.3.3

Results from the SUB perspective: white females vs. males

Sexual dimorphism between white females and males was seen in Figure 6.27, as they appeared in different quadrants of a four-quadrant grid. The subsequent statistical significance between the sexes was quantified by Goodall's F-statistic in Table 6.17. Sexual dimorphism in this perspective was evident. Females and males were thus compared independently in order to visualize these sexually dimorphic changes in the SUB perspective to observe any differences between this particular sample population and the black population sample analyzed above. Figure 6.33 demonstrates the thin-plate spline in deformation mode between females and males, which demonstrates the deviation males have from a perfect perpendicular grid (the female mean). Deformation in Figure 6.33 was seen primarily in the homologous landmarks placed along the subpubic angle. Other homologous landmarks assigned to this feature appeared to be similar between sexes, as illustrated by portions of the grid that were unaffected by deformation. Figure 6.34 subsequently shows the thin-plate spline in vector mode, which illustrates the magnitude and direction of differences between white females and white males from the SUB perspective. In Figure 6.34 the points (or circles) represent the first shape represented (white female) while the arrows represent the direction of the white male shape.

As seen in Figure 6.34, those landmarks that denote the margin of the pubis (landmarks 14-18) appear to be placed more superiorly in the white male pelvis. This result was similar to that in the black sample. In addition, the homologous points that delineate the shape of the subpubic angle and subpubic concavity (landmarks 19, 21, 23, 25 and 26) migrate closer to the medial portion of the pelvis, causing the white male subpubic concavity to be short and stout, with no projection or angling. The white female subpubic concavity, in contrast, would appear more elongated and

lengthened throughout this region, a feature that is mirrored in the non-metric visual morphology in females.

White female specimens were correctly categorized 97% of the time, (56/ 58) when compared to white males (Table 6.20). White male specimens were also classified at a 97% accuracy rate (70/ 72). The significance value obtained by the canonical variates analysis (163.348) was greater than the critical value of chi square distribution at the significance value of 0.05 with 48 degrees of freedom (65.171). The classification accuracy was high for both white females and white males, thus showing that the sexual dimorphism in this population was quantifiable when using geometric morphometrics in the SUB perspective.

Each population, as well as the combined data for both sexes, exhibited marked sexual dimorphism from the SUB perspective. Thus sexual dimorphism could be quantified, and correct classification of males and females was performed at a high rate of accuracy, regardless of the biological affiliation. This confirmed ample evidence that the subpubic angle and the subpubic concavity were sexually dimorphic between females and males. Results from this study now show that these features can be quantified successfully by employing geometric morphometrics.

6.3.4

Sexual dimorphism and the onset of age: SUB perspective

A quantifiable difference between males and females in both populations was observed when applying geometric morphometrics to the SUB perspective. This feature was thus shown to be sexually dimorphic on a statistically significant level. Analyses were then performed in order to discern if characteristics from this perspective changed with the onset of age. Thus, each group and both sexes were further categorized as "young" (50 years of age or younger) and "old" (over 50 years of age). This provided an amalgamation of eight groups: young black females, young

white females, old black female lack males, young white males, old black males and old white males.

A consensus relative warp analysis on all eight possible groups for the SUB perspective was performed to visualize the groupings between each combination of the sample (Figure 6.35). All eight permutations (1. young black female, 2. young white female, 3. old black female, 4. old white female, 5. young black male, 6. young white male, 7. old black male, 8. old white male) separate into distinctive groupings. Females of each *age* group clustered together. Males grouped with population affinity. Males and females were distinctly separated on either side of the y-axis, and this indicated that the quantification of the SUB perspective was sexually dimorphic. Young females were observed in the lower right quadrant, while old females presented in the top right quadrant of the grid. This indicated that morphology changes between all females as they advance through age. Males grouped in separate quadrants based on population affinity, and not age. This indicated that morphology was similar according to biological affiliation, and the male pelvis within the subpubic concavity region changed very little with the onset of age.

6.3.5

Sexual dimorphism and the onset of age: black females and males

Evidence represented in Figures 6.27 and 6.35 show that differences exist between black males and females, and that morphology of the pelvis from the SUB perspective varied between the age groupings of "young" and "old" for females, but varied minimally for males. To quantify and compare these differences and similarities between sexes, consensus thin-plate splines in vector mode were created for black females and black males independently to observe the differences between young and old consensus shapes.

Figure 6.36 is the thin-plate spline in vector mode that exemplifies the changes black females underwent with the onset of age. The surface of the pubis

(landmarks 14 through 18) appeared to extend superiorly with age and in this instance, also appeared to "retract" dorsally, shortening the length of the pubis. Landmarks 22, 24, 27 and 28 were broader in the ischium of old females as compared to the position of the young female landmarks. Landmarks denoting the obturator foramen appeared to change minimally. The changes along the ischium were indicative of changes seen in male pelves, thus suggesting the possibility that black females exemplify more male morphology as age increases.

The changes that occur with age in black males can be seen in Figure 6.37. This graph shows the vector mode for males as it transforms from "young" to "old" morphology. As seen in Figure 6.37, differences between young and old males existed along the pubic bone and the ischium. With this graph, changes were seen as a shortening of the pubis by the points located there (landmarks 14-18) contracting dorsally, and a broadening of the ischium through the area of the ischial tuberosity, as the points located there (landmarks 22, 24, 27 and 28) expanded out past the young black male points. When comparing the two graphs between sexes (Figures 6.36 and 6.37) the landmarks located directly below the inferior pubic symphysis that defined the subpubic angle and subpubic concavity (landmarks 19, 21, 23, 25 and 26) were distributed wider along the length of the bone in females. The same landmarks in the male sample appeared closer together and more "crowded" along the length of the bone. The changes along the subpubic concavity and ischium were indicative of changes seen in other male pelves samples in this study, thus indicating the possibility that black males demonstrated more male morphology as age increases.

Changes in black males and females with the onset of age were observable by viewing the direction and magnitude of change in thin-plate spline vector mode analyses (Figures 6.36 and 6.37). In addition, Goodall's F-statistic comparing the young (young black females vs. young black males) and the old(old black females vs. old black males) was significant for both groups (Goodall's F-statistic for the young

sample = 24.64, df = 30, p = 0.000<0.05; Goodall's F-statistic for the old sample = 14.30, df = 30, 0.000<0.05). This is illustrated in Table 6.21. Because changes were seen with age, the classification accuracy of both young and old individuals was calculated to determine if this accuracy rate decreased with the aging morphology of the black South Africans.

Table 6.22 illustrates the classification accuracy between males and females of both age groups. As can be seen in this table, young black individuals were classified at a high rate of accuracy when compared to each other (98% accurate for young black females, 100% accurate for young black males). The high classification rate between young females and young males indicated that males, when grouped in a young age category, exhibit marked male morphology which is easily quantifiable and discernable from standard female morphology. Classification accuracy decreased with the onset of age when old black females were compared to old black males (93% and 100%, respectively). This assessment of changes occurring with age may indicate that as the black females gets older, the classic "male" and "female" morphology of the pelvis became less sexually dimorphic, and thus a lower percentage of females may be correctly classified. As seen in Figure 6.36, female morphology appeared to exhibit the same differences (or undergo the same changes) as male morphology with the onset of age. Figure 6.35 illustrated this result by showing old black females closer to the male groupings on the left of the y-axis than any other of the female age/ ancestry groups. Sexual dimorphism was observed in the SUB perspective, and canonical variates analysis was able to categorize each age group with accuracy. Classification accuracies for black females and males declined with age; however, the classification accuracies are so high, that accuracy was maintained between the young and the old samples.

6.3.6

Sexual dimorphism and the onset of age: white females and males

Evidence represented in Figures 6.27 and 6.35 showed that differences existed between white males and females. Morphology of the subpubic angle from the SUB perspective appeared to not differ greatly between young and old white males. However, females exhibited distinct clusters defined by age, and not population affinity. As was seen in the previous section, this influenced the classification accuracy of old black females. Refer to Figure 6.35 for a summary of the clustering exhibited by all eight permutations in the SUB perspective. Consensus thin-plate splines in vector mode were created for white females and males to observe the differences between young and old consensus shapes.

Figure 6.38 is the thin-plate spline in vector mode that exemplified the changes white females underwent with the onset of age. The thin-plate spline in vector mode showed that little movement of homologous landmarks took place between the comparison of young and old white females. The landmarks quantifying the length of the pubis (14-18) appeared to rise superiorly in older females, causing the pubis to exhibit a thicker shape through the superior pubic region. Landmarks placed on the ischium (specifically landmarks 22, 24, and 28) appeared to be located in a more inferior position in older females, which suggested the ischium would be thicker and stouter through this region in the old females. Landmarks placed around the morphology of the obturator foramen did not appear to diverge with age. In addition, the elongated "rectangular" feature of the subpubic concavity in females did not change with age. In general, the morphological features of the subpubic angle and the subpubic concavity appeared to stay largely the same with the onset of age in the white female pelvis.

Young white males and old white males did exhibit morphological differences, as seen in the relative warp analysis in Figure 6.35. To visualize these differences, a

thin-plate spline was created in vector mode to observe the location and direction of variation between the young and old white male SUB perspective. The changes that occur with age in males can be seen in Figure 6.39. This graph shows the vector mode for males as it transforms from "young" morphology to "old" morphology.

Figure 6.39 indicated change around the periphery of the SUB view, as exemplified by distinct changes occurring in the pubic bone and the subpubic angle. Landmarks assigned to the span of the pubis (14 through 18) appeared to lengthen and expand towards the pubic symphysis, which would create a longer but thicker pubic region. The superior ischial region (landmarks 19, 21, 23, 25, and 26) migrated inferiorly between young (the point) and old males (the boundary of the arrow). These differences would change the shape of the superior subpubic region by elongating this area to an extent in the old white male population. Finally, landmarks 22, 24, 27 and 28 contracted inward, towards the obturator foramen, which created a thinner ischial margin. This may indicate a movement towards a more "female" appearing ischial region.

Changes in white males and females with the onset of age were observable by viewing the direction and magnitude of change in thin-plate spline vector mode analyses (Figures 6.38 and 6.39). Goodall's F-statistic comparing the young (young white females vs. young white males) and the old (old white females vs. old white males) resulted in differing statistical outcomes. Table 6.23 illustrates that differences between young females and males are insignificant (Goodall's F-statistic = 8.13, df = 48, 0.083>0.05), while the differences between old females and males in the SUB perspective are, in fact, statistically significant. The significance in the statistic increased with the old sample (Goodall's F-statistic = 23.65, df = 48, 0.000<0.05). Because of these discrepancies and the apparent variability of male morphology in the young white male SUB perspective, the classification accuracies of both young and old individuals were calculated to determine if this accuracy rate increased with the aging morphology of white South Africans.

Table 6.24 illustrates the classification accuracy between males and females of both age groups. As can be seen in this table, canonical variates analysis from the IMP statistical package could not correctly distinguish young white females from young white males with the SUB perspective; no statistics were generated when the analysis was performed. This indicated that the morphology of the SUB perspective with these two groups compared was the same.

The small sample size for young white individuals (11 for females, 23 for males) may have played a role in the canonical variates analysis results being unable to perform the analysis. However, the variability in morphology of the young white male pelvis may have influenced the lack of differences seen when comparing young white females to young white males. Male os coxae in this group appeared to exhibit either inconsistent male pelvic morphology, or exhibited pelvic morphology that has been historically (and with other populations) attributed to females. In other words, young white males and females appeared to have largely the same pelvic morphology through the characteristics of the SUB perspective.

Classification accuracy in the old sample provided accurate results, however. Old white females were classified correctly 98% of the time when compared to their old male counterparts. The old males were also classified at a rate of 98% accuracy. This assessment of changes occurring with age may indicate that as white South Africans get older, the classic "male" and "female" morphology of the pelvis changes dramatically in its degree of sexual dimorphism. Old females and males exhibited quantifiable characteristics in the SUB perspective, allowing for old females to be categorized correctly when compared to old males. Sexual dimorphism was present in the older group.

Although females and males from different ancestries exhibited differing rates of classification accuracy, the SUB perspective was still observed to be a highly accurate indicator of sex when the shape of the subpubic angle and the subpubic concavity were quantified, and males and females were compared to each other.

Thus the SUB perspective was deemed sexually dimorphic. However, unusual results with the young white sample population and the inability of the CVA program to correctly categorize males from females in this sample illustrated a peculiar divergence in this sample that is neither expected nor a classic divergence based on sexual dimorphism. White South Africans did not conform to the classic tenets of sexual dimorphism as seen in other populations.

6.4

Sexual dimorphism in the pelvis: SCI perspective

Five homologous landmarks were assigned to the portion of the pelvic bone as shown in Figure 3.29. The SCI perspective quantified characteristics of the greater sciatic notch through landmark data analysis. Confirmation of the sexually dimorphic nature in the SCI perspective was achieved; the presence of sexual dimorphism in this skeletal element is illustrated in Figure 6.40.

As can be seen, a sexually dimorphic component existed with the SCI perspective, as well as a population component between sexes. All females were viewed to group to the left of the y-axis and within the upper left hand quadrant of the grid. All males were viewed to the right of the y-axis, while males from each population presented in different quadrants on the right-hand side of the grid. Males, although on the same side of the y-axis, appeared to diverge dramatically from each other, indicating a difference in morphology between groups. In addition, white males were observed to be quite close to the nearest female consensus, the black females. This initially indicated that the SCI perspective and its quantified morphology might be distinct between males and females. In addition, population groups in males appeared to separate into different morphological forms as well, with white males presenting fairly close to the black female SCI consensus shape. Females appeared more congruent with each other across ancestry types

6.4.1

Results from the SCI perspective between females and males

Figure 6.40 illustrates the differences between females and males. Statistical analyses in the form of Goodall's F test from the IMP TwoGroup statistical package was performed to quantify the magnitude of differences between the above four groups. Goodall's F-test assesses inter-group shape disparity between groups, taking sample variance into account. Analyses were performed to observe the magnitude of these differences. Table 6.25 illustrates the differences between all groups compared in Figure 6.40. All groups were observed to be sexually dimorphic on a statistically significant level with the SCI perspective.

Table 6.25 confirmed the results visualized in Figure 6.40. Males and females appear to be sexually dimorphic on a significant level, as observed by their separation in the consensus relative warp grid. Males and females, regardless of their population, appeared distinctly apart from each other. Females appeared closer together in consensus morphology than their male counterparts; it appeared as if black and white males differed considerably in their anatomical features when the consensus relative warp grid was assessed. In addition, black females and males may be more sexually dimorphic than their white counterparts, based on the comparative Goodall's F-statistic (white females and males Goodall's F-statistic = 46.04, black females and males Goodall's F-statistic = 60.28). Both, however, were significantly different enough to deem the SCI perspective and the shape of the greater sciatic notch sexually dimorphic.

A reference consensus thin-plate spline was created to view the mean shape of all the individuals in the sample for the SCI perspective. Figure 6.41 is a representation of the average shape of the males and females exemplified by an exactly perpendicular grid. Figure 6.42 demonstrates the thin-plate spline for the deformation from the SCI perspective. The deformation grid exemplifies the areas of

form breakdown from the perpendicular reference, in this case the female shape. The female shape would have appeared as a perfect perpendicular grid, and this figure now gives the degree and deformation of the males on this female/ reference grid. The deformation grid exhibited a large amount of warping and collapse along the locations where all five homologous landmarks were placed. Figure 6.43 demonstrates the differences exhibited between females and males in thin-plate spline vector mode. In Figure 6.43 the points (or circles) represent the first shape represented (female) while the arrows represent the direction of the male shape.

As seen in Figures 6.42 and 6.43, discrepancy between females (the point of origin of the arrow in vector mode) and males (the end length of the arrow in vector mode) existed in the location of the inferior ischial spine, the location of the outer point of the greater sciatic notch, before the pelvis curves back towards the auricular surface, and the depth of the greater sciatic notch itself. The vector mode thin-plate spline illustrated numerous differences between males and females in the pelvic morphology of the greater sciatic notch (Figure 6.43). Females (represented by the point) exhibited a more elongated and extended greater sciatic notch surface through the curvature towards the auricular surface than their male counterparts (represented by the boundary of the arrow). Males appeared short and truncated along this margin. These differences are illustrated through landmarks 2, 3 and 4. In contrast, male morphology appeared to extend longer than female morphology along the inferior border of the greater sciatic notch, which included the curvature towards the inferior ischial spine (landmark 5) and the landmark placed on the inferior ischial spine itself (landmark 1). Landmark 2 is the point of maximum curvature in the sciatic notch. This region is seen to extend or "depress" the greater sciatic notch further inward with males than with females. This may result in the deep, narrow greater sciatic notch width seen visually in male morphology. The shallow position of landmark 2 in females may account for the wider, shallower morphology of females. It was interesting to note that the major differences are not in the width of the greater

sciatic, notch, but rather in its a "legs" were seen to be significantly different in length.

The accuracy by which these differences in the pelvis can assign a specimen was assessed by means of a canonical variates (CVA) analysis. Table 6.26 represents the accuracies obtained from this analysis. Female specimens were correctly categorized 70% of the time, (105/ 151) while male specimens were categorized correctly 79% of the time (142/ 180). The p-value obtained by the canonical variates analysis (132.160) was greater than the critical value of chi square distribution at the significance value of 0.05 with two degrees of freedom (5.991). This indicated that the SCI perspective, which included a quantitative observation of the greater sciatic notch, was moderately sexually dimorphic.

Morphology of the greater sciatic notch between the members of each group (females and males) was different, and correct classification of females vs. males was performed on a statistically significant level. However, the classification accuracy based on quantified morphology of the greater sciatic notch in the South African population is lower than other features used to determine sex from the human skeleton.

6.4.2

Results from the SCI perspective: black females vs. males

Sexual dimorphism between black females and males was initially shown in Figure 6.40, and the statistical significance between the sexes was quantified by Goodall's F-statistic in Table 6.25. Sexual dimorphism in this perspective appeared more statistically significant in black South Africans than in white South Africans. Black females and males were thus compared independently to visualize sexually dimorphic changes in the SCI perspective.

Figure 6.44 demonstrates the thin-plate spline in deformation mode, and Figure 6.45 is the thin-plate spline in vector mode. As was the case before, in Figure

6.45 the points (or circles) represent the first shape represented (black females) while the arrows represent the direction of the black male shape.

The most deformation between black females and males occurred at the margins of the greater sciatic notch. These deformations between females (as the reference) and males (as the deformation) "tilted" the graph downwards on the right-hand (inferior) margin. The two sexes differ in that males exhibited a shortened, truncated greater sciatic notch margin along the superior border (landmarks 2, 3, and 4) and appear extended along the inferior border (landmarks 1 and 5). In addition, the position of landmark 2, the point of most curvature of the greater sciatic notch, appears deeper within the notch of the black male than within the notch of the female.

Table 6.27 represents the accuracies obtained from the canonical variates analysis. Black females were correctly categorized 78% of the time (71/ 91) while males 86% (90/ 105). The significance value obtained by the canonical variates analysis (94.637) was greater than the critical value of chi square distribution at the significance value of 0.05 with two degrees of freedom (5.991). The classification accuracy was high enough for both males and females to show moderate sexual dimorphism, which was quantifiable when using geometric morphometrics from the SCI perspective.

6.4.3

Results from the SCI perspective: white females vs. males

Sexual dimorphism between white females and males was seen first in Figure 6.40 as a relative warp analysis separated each sex and population. White females and males appeared in different quadrants of a four-quadrant grid. The subsequent statistical significance between the sexes was quantified by Goodall's F-statistic in Table 6.25. Sexual dimorphism existed in this perspective.

Figure 6.46 demonstrates the thin-plate spline in deformation mode between females and males, which demonstrates the deviation males have from a perfect perpendicular grid (the female mean). Deformation in Figure 6.46 was seen primarily in position of the inferior and superior landmarks of the greater sciatic notch, as well as the depth of the notch itself when comparing females to males. Other homologous landmarks assigned to this feature appeared to be similar between male and female morphology, as illustrated by portions of the grid that were unaffected by deformation. Figure 6.47 subsequently shows the thin-plate spline in vector mode, which illustrates the magnitude and direction of differences between white females and white males from the SCI perspective

As seen in Figure 6.47, those landmarks that denote the outer margins of the greater sciatic notch differ from females (the circles) to males (the arrow boundaries). Landmark 1 (which indicated the most projecting point of the inferior ischial spine) was positioned in a wider and shorter region in females than in males. Landmark 1 in males was placed in a more extended position, but also appeared to decrease the visual width of the greater sciatic notch by being positioned closer to landmark 3. Landmark 3, in contrast, appeared to be positioned in a wider, more extended, and more superiorly location in females than in males. Landmark 3 in males was positioned closer within the notch itself and in a location that would shorten the length between landmark 3 and 4. Landmark 2, the point of maximum curvature of the greater sciatic notch, appeared shallow in females and deeper within the notch in males. Landmarks 4 and 5 did not exhibit any remarkable differences in placement between white females and white males. These two landmarks would delineate the actual width of the greater sciatic notch margins. Because they appear congruent between males and females, this indicated that the morphology of the actual width of the notch was similar between the sexes.

The accuracy by which these differences in the greater sciatic notch region can assign white specimens was assessed by means of a canonical variates (CVA)

analysis (Table 6.28). White female specimens were correctly categorized 80% of the time(48/ 60) and males 87% (65/ 75). The significance value obtained by the canonical variates analysis (85.785) was greater than the critical value of chi square distribution at the significance value of 0.05 with two degrees of freedom (5.991). The classification accuracy was significant for both white females and white males, thus showing that the sexual dimorphism in this population was quantifiable when using geometric morphometrics in the SCI perspective.

Each population, as well as the combined data of all females and all males, exhibited marked sexual dimorphism from the SCI perspective. Thus sexual dimorphism could be quantified, and correct classification of males and females was performed for all males and females, and for each population group. This confirmed ample evidence that the morphology of the greater sciatic notch was sexually dimorphic between females and males. Results from this study show that these features can be quantified successfully by employing geometric morphometrics.

6.4.4

Sexual dimorphism and the onset of age: SCI perspective

A quantifiable difference between males and females in both populations was observed when applying geometric morphometrics to the SCI perspective, a view that exemplifies the greater sciatic notch of the pelvis. This feature was thus shown to be sexually dimorphic on a statistically significant level. Analyses were then performed in order to discern if characteristics from this perspective changed with the onset of age. Thus, each population group and both sexes were further categorized as "young" (50 years of age or younger) and "old" (over 50 years of age) as seen before. The differences between males and females from each age group were subsequently examined.

A consensus relative warp analysis on all eight possible groups for the SCI perspective was performed to visualize the groupings between each combination of the sample (Figure 6.48). This figure illustrates the complex morphology of this

pelvic region. All females were observed on the right side of the y-axis, indicating a distinctive sexually dimorphic component. Most males (young black males, old black males, and old white males) clustered to the left of the y-axis. This, again, indicated that the quantification of the SCI perspective was sexually dimorphic. Most females (young white females, old black females, and old white females) were observed in the upper right quadrant, while young black females presented in the bottom right quadrant of the grid, and grouped most closely with the morphology of young white males.

Old black and white females clustered together, and old black and white males clustered together. Further, it appeared as if old black male and old white male morphology was indistinguishable from each other. This indicated a morphological change between all males and females to some extent as they advanced through age. The biological affiliation of each group did not seem to be a discriminating factor. Black population groups and white population groups clustered together. This indicated that morphology was similar according to age.

6.4.5

Sexual dimorphism and the onset of age: black females and black males

Evidence represented in Figures 6.40 and 6.48 show that differences exist between black males and females, and that morphology of the pelvis from the SCI perspective varied between the age groupings of "young" and "old" for both males and females. To quantify and compare these differences and similarities between sexes, consensus thin-plate splines in vector mode were created for black females and black males independently to observe the differences between young and old consensus shapes.

Figure 6.49 is the thin-plate spline in vector mode that exemplifies the changes black females underwent with the onset of age. Landmarks 1, 2 and 3 show quantifiable changes from young black females to old black females. Landmark 1 appears to be in a wider and more anterior position in old black females than in

young black females; this change would create a shorter but wider sciatic notch. Landmark 3, in contrast, projects inward toward the middle of the notch with the onset of age, producing a narrower notch for old black females. In addition, landmark 2 (the location of maximum curvature of the greater sciatic notch) was seen to be in a more superior position in old black females than in young black females. Landmarks 4 and 5 did not appear to migrate or deviate from their original positions between young black females and old black females.

The changes that occur with age in black males can be seen in Figure 6.50. This graph shows the vector mode for black males as it transforms from "young" morphology to "old" morphology in the SCI perspective. As seen in Figure 6.50, differences between young black males and old black males existed along the entire margin of the greater sciatic notch. All landmarks in the old male SCI perspective migrated around the sciatic notch. Landmarks 1 and 5 showed a slight migration inward, toward the medial section of the greater sciatic notch space. Landmarks 3 and 4 positioned themselves more towards landmark 2, the location of maximum sciatic notch curvature in old black males. This would have created a shorter, more truncated greater sciatic notch morphology in old black males than in young black males.

Changes in black males and females with the onset of age were observable by viewing the direction and magnitude of change in thin-plate spline vector mode analyses (Figures 6.49 and 6.50). In addition, Goodall's F-statistic comparing the young black sample (young black females vs. young black males) and the old black sample (old black females vs. old black males) was significant for both groups (Goodall's F-statistic for the young sample = 30.22, df = 2, $p = 0.000<0.05$; Goodall's F-statistic for the old sample = 32.50, df = 2, $0.000<0.05$) as seen in Table 6.29. Because changes were seen with age, the classification accuracy of both young and old individuals was calculated to determine if this accuracy rate decreased with the aging morphology of the black population.

Table 6.30 illustrates the classification accuracy between males and females of both age groups. Young black individuals were classified with accuracy when compared to each other (80% accurate for young black females, 85% for young black males). Classification accuracy remained basically the same with the onset of age when old black females were compared to old black males (81% and 84%, respectively). Assessment of classification accuracies between young and old age groups with the black population indicated that the classic "male" and "female" morphology of the pelvis maintained its sexually dimorphic nature throughout the onset of advanced age. Figure 6.48 showed old black females closer to the male groupings on the left of the y-axis than any other of the female age/ population groups. This could indicate a slight variance to more "male" morphology with the black female pelvis, although classification accuracies did not decrease with this sample, they increased. Regardless, sexual dimorphism was observed in the SCI perspective, and canonical variates analysis was able to categorize each age group with accuracy. Changes with age to the SCI perspective did not adversely influence the classification accuracy for females or males in this population group; as the age increased with black females and males, the ability to correctly assign a female specimen to its correct group remained virtually the same.

6.4.6

Sexual dimorphism and the onset of age: white females and males

Evidence represented in Figures 6.40 and 6.48 showed that differences existed between white males and females in the SCI perspective. Morphology of the greater sciatic notch appeared to differ greatly between young white male individuals and old white male individuals based on the separation of the two consensuses in the relative warp graph shown in Figure 6.48. Changes appeared to be taking place in the white male pelvis with age. Females in this same graph exhibited distinct clusters defined only by sex, and not population affinity. Consensus thin-plate

splines in vector mode were created for white females and white males to observe the differences between young and old consensus shapes.

Figure 6.51 is the thin-plate spline in vector mode that exemplified the changes white females underwent with the onset of age. The thin-plate spline in vector mode showed that little movement of homologous landmarks took place between the comparison of young white females and old white females. Landmark 1 appeared to migrate superiorly, towards the surface of the pubis, and slightly inward toward the point of most curvature in the greater sciatic notch (landmark 2). This would create a shorter and wider greater sciatic notch morphology in old white females as compared to young white females. Landmark 3, the end of the sciatic notch before the bone curves backwards towards the auricular surface, was positioned in a more extended position in old white females than in young white females. This would have the opposite effect of landmark 1's movement, producing a more elongated greater sciatic notch in this location when viewing old white females.

Young white males and old white males did exhibit marked morphological differences, as seen in the relative warp analysis in Figure 6.48. To visualize these differences, a thin-plate spline was created in vector mode to observe the location and direction of variation between the young white male SCI perspective, and the old white male SCI perspective. The changes that occur with age in white males can be seen in Figure 6.52. This graph shows the vector mode for white males as it transforms from "young" morphology to "old" morphology.

Figure 6.52 indicated alteration around the periphery of the SCI view, as exemplified by distinct changes occurring in all homologous landmarks within the greater sciatic notch. Landmark 3 migrated inward towards the iliac surface and towards the greatest curvature of the notch (landmark 2), shortening this aspect of the greater sciatic notch in old white males (categorized by the boundary of the arrow), as opposed to its elongated appearance in young white males (categorized

by the point). Landmark 4 also migrated towards the interior of the pelvis, increasing this "shortening" effect. Landmarks 1 and 5, however, elongate towards the inferior margin of the ischium in old white males, which may lengthen the morphology of the greater sciatic notch in this region. Finally, landmark 2 migrated medially and toward the auricular surface, creating what may be visually construed as constriction in the point of maximum curvature.

Changes in white males and females with the onset of age were observable by viewing the direction and magnitude of change in thin-plate spline vector mode analyses (Figures 6.51 and 6.52). Goodall's F-statistic comparing the young white sample (young white females vs. young white males) and the old white sample (old white females vs. old white males) resulted in differing statistical outcomes. Table 6.31 illustrates that differences between young white females and young white males just reached statistical significance (Goodall's F-statistic = 3.29, df = 2, 0.043<0.05), while the differences between old white females and old white males in the SCI perspective are highly significant (Goodall's F-statistic = 46.41, df = 2, 0.000<0.05). Because of these discrepancies and the apparent variability of male morphology in the young white male SCI perspective (as seen in the previous section with the SUB perspective), the classification accuracies of both young and old individuals were calculated to determine if this accuracy rate increased with the aging morphology of the white population.

Table 6.32 illustrates the classification accuracy between males and females of both age groups. As can be seen in this table, young white females were categorized correctly 73% of the time, while young white males were categorized with 74% accuracy. The young white male pelvis was quite variable in morphology. This may have influenced the inability to categorize young white males from young white females with a higher degree of accuracy. A lack of morphological differences was seen when comparing young white females to young white males. Male os coxae in this group appeared to exhibit either inconsistent male pelvic morphology, or

exhibited pelvic morphology that has been historically (and with other populations) attributed to females.

Classification accuracy in the old white sample provided accurate results, however. Old white females and males were categorized at a higher rate of accuracy than their younger counterparts (84% and 89%, respectively).

The assessment of changes occurring with age may indicate that as the white population gets older, the classic "male" and "female" morphology of the pelvis changes dramatically in its degree of sexual dimorphism. Young white females, when compared to young white males, were not distinguishable enough to provide very accurate canonical variates results. Old females and males, in contrast, exhibited quantifiable characteristics in the SCI perspective, allowing for old females to be categorized correctly when compared to old white males. Sexual dimorphism was present and marked in the old white population.

Although females and males from different population groups exhibited differing rates of classification accuracy, the SCI perspective was still observed to be a highly accurate indicator of sex when the shape of the greater sciatic notch was quantified, and males and females were compared to each other. Thus the SCI perspective was deemed sexually dimorphic. However, unusual results with the young white sample population and the inability of the CVA program to correctly categorize males from females with accuracy in this sample illustrated a peculiar divergence in this sample that is neither expected nor a classic divergence based on sexual dimorphism. Male pelvic morphology in white South Africans did not concur with the classic tenets of sexual dimorphism as seen in other populations. In fact, both perspectives of the pelvis (SUB perspective and SCI perspective) exhibited problematic results. Accurate classification of young white male pelvic morphology was either difficult or impossible to achieve.

Table 6.1: Statistical significance between females and males, EPI perspective.

	Statistical significance between groups, EPI		
Group	Goodall's F-test	df	p- value
All females vs. all males	13.48	30	**0.000***
Black females vs. Black males	6.65	30	**0.000***
White females vs. White males	12.78	30	**0.000***

Significant, < 0.05

Table 6.2: Percentage of males and females correctly assigned using canonical variates analysis, EPI perspective. *N* = 347

	CVA assignment based on shape data, EPI			
Group	Correctly assigned	Incorrectly assigned	Percentage correctly assigned	Chi square value
Females (*n*=163)	129	34	79%	**148.185***
Males (*n*=184)	143	41	78%	

**** Significant, at 0.05 level***

Table 6.3: Percentage of black males and black females correctly assigned using canonical variates analysis, EPI perspective. *N* = 208

	CVA assignment based on shape data, EPI			
Group	Correctly assigned	Incorrectly assigned	Percentage correctly assigned	Chi square value
Black females (*n*=100)	83	17	83%	**110.017***
Black males (*n*=108)	92	16	85%	

Significant, at 0.05 level

Table 6.4: Percentage of white males and white females correctly assigned using canonical variates analysis, EPI perspective. *N* = 139

Group	CVA assignment based on shape data, EPI			
	Correctly assigned	Incorrectly assigned	Percentage correctly assigned	Chi square value
White females (*n*=63)	57	6	91%	
White males (*n*=76)	68	8	90%	**107.188***

Significant, at 0.05 level

Table 6.5: Statistical significance between black females and males, EPI perspective.

Group	Statistical significance between groups, EPI		
	Goodall's F-test	df	p- value
Young black females vs. Young black males	5.50	30	**0.000***
Old black females vs. Old black males	3.72	30	**0.000***

Significant at 0.05 level

Table 6.6: Percentage of young and old black males and females correctly assigned using canonical variates analysis, EPI perspective. (*n* = 106 young, *n* = 102 old)

Group	CVA assignment based on shape data, EPI			
	Correctly assigned	Incorrectly assigned	Percentage correctly assigned	Chi square value
Young black females (*n*=50)	47	3	94%	
Young black males (n=56)	50	6	89%	**85.5835***
Old black females (*n*=50)	48	2	96%	
Old black males (n=52)	49	3	94%	**100.776***

Significant, at 0.05 level

Table 6.7: Statistical significance between white females and males, EPI perspective.

	Statistical significance between groups, EPI		
Group	Goodall's F-test	df	p- value
Young white females vs. Young white males	4.44	30	**0.014***
Old white females vs. Old white males	8.80	30	**0.000***

Significant, < 0.05

Table 6.8: Percentage of young and old white males and females correctly assigned using canonical variates analysis, EPI perspective. (n = 37 young, n = 102 old)

	CVA assignment based on shape data, EPI			
Group	Correctly assigned	Incorrectly assigned	Percentage correctly assigned	Chi square value
Young white females (*n*=13)	-	-	-%	-
Young white males (n=24)	-	-	-%	
Old white females (*n*=50)	46	4	92%	**81.2308***
Old white males (n=52)	44	8	85%	

Significant, at 0.05 level

Table 6.9: Statistical significance between females and males, OL perspective.

Group	Statistical significance between groups, OL		
	Goodall's F-test	df	p- value
All females vs. all males	9.30	22	**0.000***
Black females vs. Black males	7.08	22	**0.000***
White females vs. White males	3.86	22	**0.000***

Significant, < 0.05

Table 6.10: Percentage of males and females correctly assigned using canonical variates analysis, OL perspective. *N* = 348

Group	CVA assignment based on shape data, OL			
	Correctly assigned	Incorrectly assigned	Percentage correctly assigned	Chi square value
Females (*n*=163)	135	28	83%	
Males (*n*=185)	156	29	84%	**211.344***

**** Significant, at 0.05 level***

Table 6.11: Percentage of black males and black females correctly assigned using canonical variates analysis, OL perspective. *N* = 210

Group	CVA assignment based on shape data, OL			
	Correctly assigned	Incorrectly assigned	Percentage correctly assigned	Chi square value
Black females (*n*=100)	82	18	82%	
Black males (*n*=110)	89	21	81%	**123.551***

****Significant, at 0.05 level***

Table 6.12: Percentage of white males and white females correctly assigned using canonical variates analysis, OL perspective. *N* = 138

Group	CVA assignment based on shape data, OL			
	Correctly assigned	Incorrectly assigned	Percentage correctly assigned	Chi square value
White females (*n*=63)	55	8	87%	
White males (*n*=75)	66	9	88%	**111.226***

Significant, at 0.05 level

Table 6.13: Statistical significance between black females and males, OL perspective.

Group	Statistical significance between groups, OL		
	Goodall's F-test	df	p- value
Young black females vs. Young black males	5.85	22	**0.000***
Old black females vs. Old black males	2.45	22	**0.000***

Significant, < 0.05

Table 6.14: Percentage of young and old black males and females correctly assigned using canonical variates analysis, OL perspective. (*n* = 100 young, *n* = 110 old)

Group	CVA assignment based on shape data, OL			
	Correctly assigned	Incorrectly assigned	Percentage correctly assigned	Chi square value
Young black females (*n*=50)	42	8	84%	
Young black males (n=57)	54	3	95%	**102.773***
Old black females (*n*=50)	40	10	80%	
Old black males (n=53)	45	8	85%	**56.400***

Significant, at 0.05 level

Table 6.15: Statistical significance between white females and males, OL perspective.

Group	Statistical significance between groups, OL		
	Goodall's F-test	df	p- value
Young white females vs. Young white males	1.79	22	**0.022***
Old white females vs. Old white males	3.32	22	**0.000***

Significant, < 0.05

Table 6.16: Percentage of young and old white males and females correctly assigned using canonical variates analysis, OL perspective. (*n* = 35 young, *n* = 102 old)

Group	CVA assignment based on shape data, OL			
	Correctly assigned	Incorrectly assigned	Percentage correctly assigned	Chi square value
Young white females (*n*=13)	12	1	92%	**35.477***
Young white males (n=23)	23	0	100%	
Old white females (*n*=50)	45	5	90%	**78.459***
Old white males (n=52)	47	5	90%	

Significant, at 0.05 level

Table 6.17: Statistical significance between females and males, SUB perspective.

Group	Statistical significance between groups, SUB		
	Goodall's F-test	df	p- value
All females vs. all males	61.72	48	**0.000***
Black females vs. Black males	36.59	48	**0.000***
White females vs. White males	30.09	48	**0.000***

Significant, < 0.05

Table 6.18: Percentage of males and females correctly assigned using canonical variates analysis, SUB perspective. *N* = 318

Group	CVA assignment based on shape data, SUB			
	Correctly assigned	Incorrectly assigned	Percentage correctly assigned	Chi square value
Females (*n*=143)	135	8	94%	
Males (*n*=175)	165	10	94%	**397.806***

Significant, at 0.05 level

Table 6.19: Percentage of black males and black females correctly assigned using canonical variates analysis, SUB perspective. *N* = 188

Group	CVA assignment based on shape data, SUB			
	Correctly assigned	Incorrectly assigned	Percentage correctly assigned	Chi square value
Black females (*n*=85)	82	3	96%	
Black males (*n*=103)	101	2	98%	**262.356***

Significant, at 0.05 level

Table 6.20: Percentage of white males and white females correctly assigned using canonical variates analysis, SUB perspective. *N* = 130

Group	CVA assignment based on shape data, SUB			
	Correctly assigned	Incorrectly assigned	Percentage correctly assigned	Chi square value
White females (*n*=58)	56	2	97%	
White males (*n*=72)	70	2	97%	**163.348***

Significant, at 0.05 level

Table 6.21: Statistical significance between black females and males, SUB perspective.

Group	Statistical significance between groups, SUB		
	Goodall's F-test	df	p- value
Young black females vs. Young black males	24.64	48	**0.000***
Old black females vs. Old black males	14.30	48	**0.000***

Significant, < 0.05

Table 6.22: Percentage of young and old black males and females correctly assigned using canonical variates analysis, SUB perspective. (*n* = 96 young, *n* = 92 old)

Group	CVA assignment based on shape data, SUB			
	Correctly assigned	Incorrectly assigned	Percentage correctly assigned	Chi square value
Young black females (*n*=41)	40	1	98%	
Young black males (n=55)	55	0	100%	**165.780***
Old black females (*n*=44)	41	3	93%	
Old black males (n=48)	48	48	100%	**112.469***

Significant, at 0.05 level

Table 6.23: Statistical significance between white females and males, SUB perspective.

	Statistical significance between groups, SUB		
Group	Goodall's F-test	df	p- value
Young white females vs. Young white males	8.13	48	0.083
Old white females vs. Old white males	23.65	48	**0.000***

Significant, < 0.05

Table 6.24: Percentage of young and old white males and females correctly assigned using canonical variates analysis, SUB perspective. (*n* = 34 young, *n* = 96 old)

	CVA assignment based on shape data, SUB			
Group	Correctly assigned	Incorrectly assigned	Percentage correctly assigned	Chi square value
Young white females (*n*=11)	-	-	-%	-
Young white males (n= 23)	-	-	-%	
Old white females (*n*=47)	46	1	98%	**122.405***
Old white males (n=49)	48	1	98%	

Significant, at 0.05 level

Table 6.25: Statistical significance between females and males, SCI perspective.

	Statistical significance between groups, SCI		
Group	Goodall's F-test	df	p- value
All females vs. all males	88.85	2	**0.000***
Black females vs. Black males	60.28	2	**0.000***
White females vs. White males	46.04	2	**0.000***

Significant, < 0.05

Table 6.26: Percentage of males and females correctly assigned using canonical variates analysis, SCI perspective. *N* = 331

	CVA assignment based on shape data, SCI			
Group	Correctly assigned	Incorrectly assigned	Percentage correctly assigned	Chi square value
Females (*n*=151)	105	46	70%	
Males (*n=180*)	142	38	79%	**132.160***

**** Significant, at 0.05 level***

Table 6.27: Percentage of black males and black females correctly assigned using canonical variates analysis, SCI perspective. *N* = 196

	CVA assignment based on shape data, SCI			
Group	Correctly assigned	Incorrectly assigned	Percentage correctly assigned	Chi square value
Black females (*n*=91)	71	20	78%	
Black males (*n*=105)	90	15	86%	**94.637***

Significant, at 0.05 level

Table 6.28: Percentage of white males and white females correctly assigned using canonical variates analysis, SCI perspective. *N* = 135

Group	CVA assignment based on shape data, SCI			
	Correctly assigned	Incorrectly assigned	Percentage correctly assigned	Chi square value
White females (*n*=60)	48	12	80%	
White males (*n*=75)	65	10	87%	**85.785***

Significant, at 0.05 level

Table 6.29: Statistical significance between black females and males, SCI perspective.

Group	Statistical significance between groups, SCI		
	Goodall's F-test	df	p- value
Young black females vs. Young black males	30.22	2	**0.000***
Old black females vs. Old black males	32.50	2	**0.000***

Significant, < 0.05

Table 6.30: Percentage of young and old black males and females correctly assigned using canonical variates analysis, SCI perspective. (*n* = 98 young, *n* = 98 old)

Group	CVA assignment based on shape data, SCI			
	Correctly assigned	Incorrectly assigned	Percentage correctly assigned	Chi square value
Young black females (*n*=44)	35	9	80%	
Young black males (n=54)	46	8	85%	**44.457***
Old black females (*n*=47)	38	9	81%	
Old black males (n=51)	43	8	84%	**50.449***

Significant, at 0.05 level

Table 6.31: Statistical significance between white females and males, SCI perspective.

Group	Statistical significance between groups, SCI		
	Goodall's F-test	df	p- value
Young white females vs. Young white males	3.29	2	**0.043***
Old white females vs. Old white males	46.41	2	**0.000***

**Significant, < 0.05*

Table 6.32: Percentage of young and old white males and females correctly assigned using canonical variates analysis, SCI perspective. (*n* = 34 young, *n* =101 old)

Group	CVA assignment based on shape data, SCI			
	Correctly assigned	Incorrectly assigned	Percentage correctly assigned	Chi square value
Young white females (*n*=11)	8	3	73%	
Young white males (n=23)	17	6	74%	11.677
Old white females (*n*=49)	41	8	84%	
Old white males (n=52)	46	6	89%	**73.503***

Significant, at 0.05 level

Figure 6.1: Consensus relative warp analysis of females and males, EPI perspective.

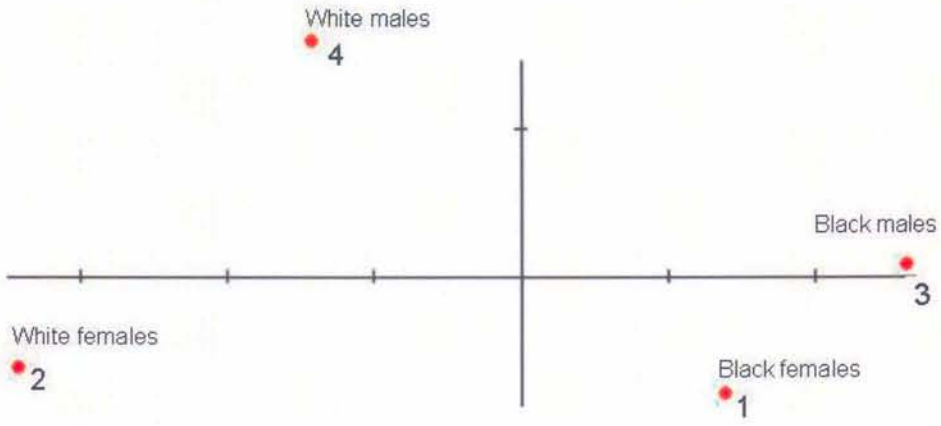

Figure 6.2: Consensus thin-plate spline reference shape of all females and all males from the EPI perspective.

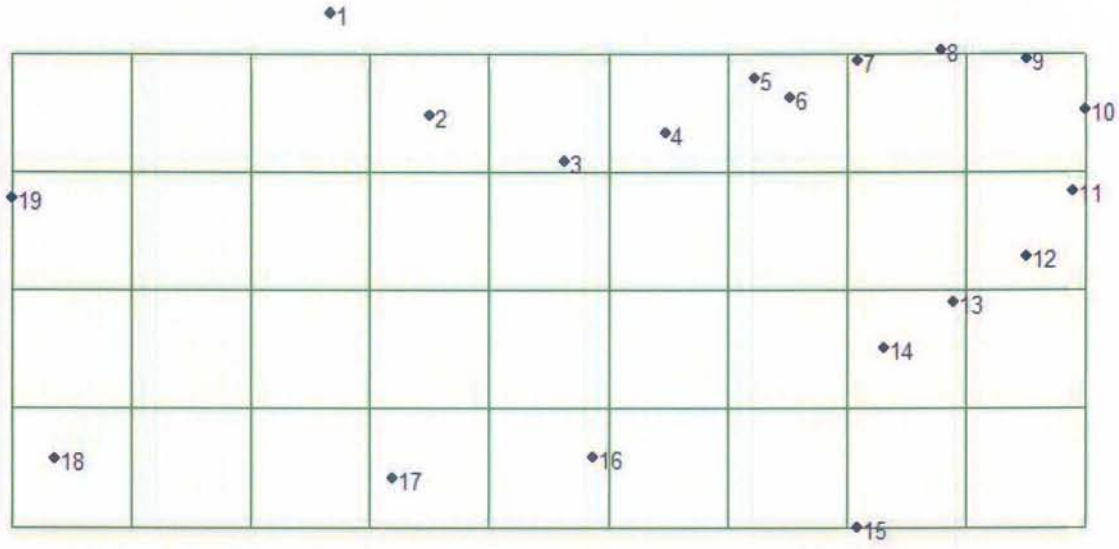

Figure 6.3: Consensus thin-plate spline in deformation mode demonstrating the differences between the reference shape (all females) and all males, EPI perspective.

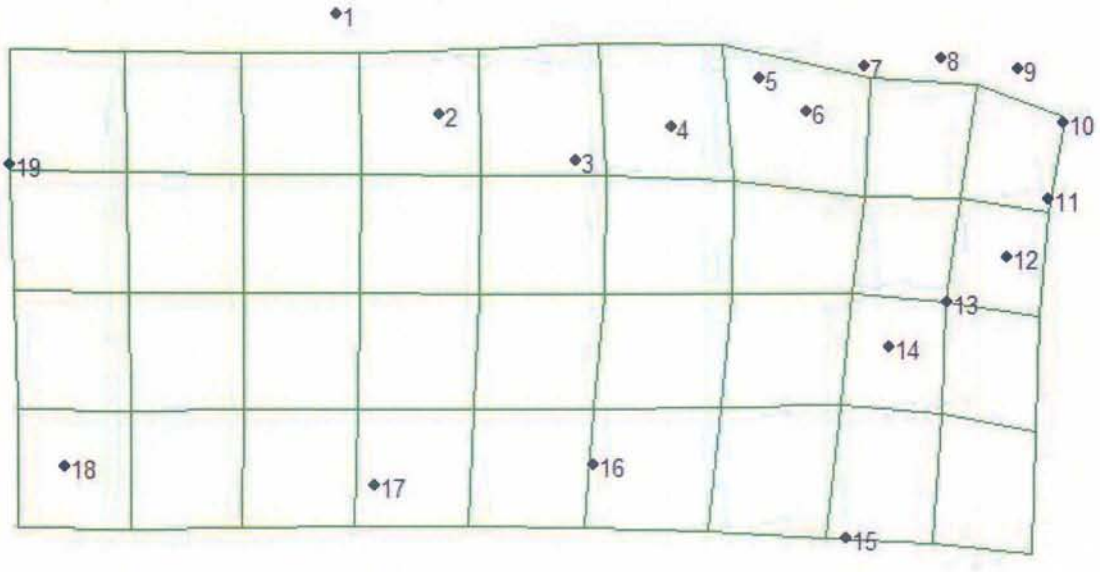

Figure 6.4: Consensus thin-plate spline (in vector mode) demonstrating the differences between all females and all males, EPI perspective.

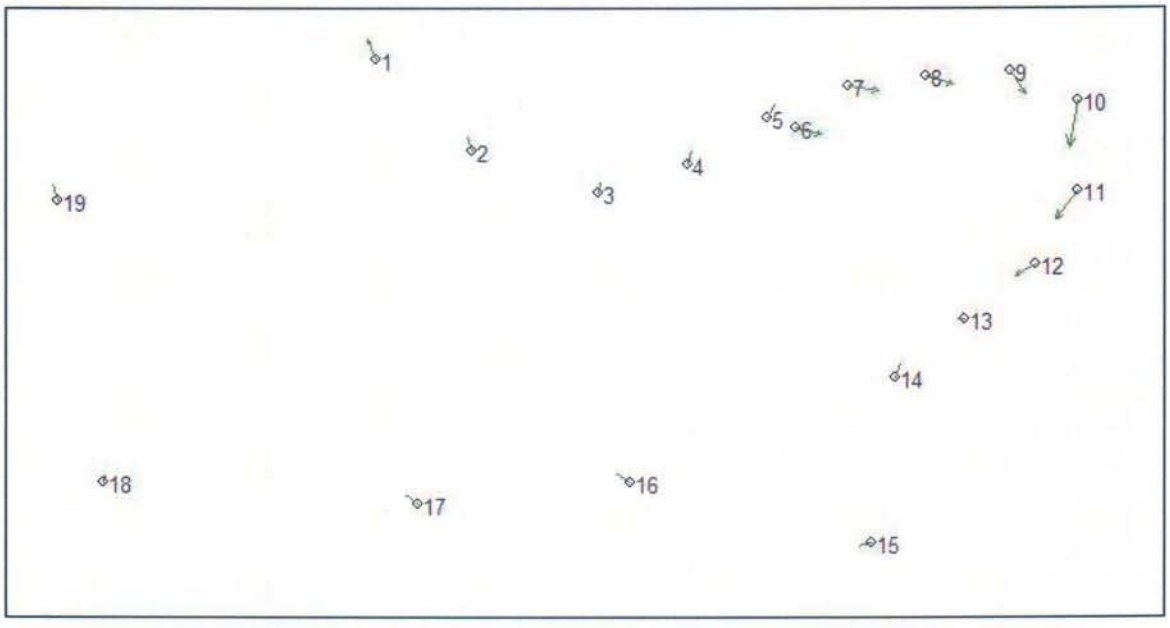

Figure 6.5: Consensus thin-plate spline in deformation mode demonstrating the differences between the reference shape (black females) and black males, EPI perspective.

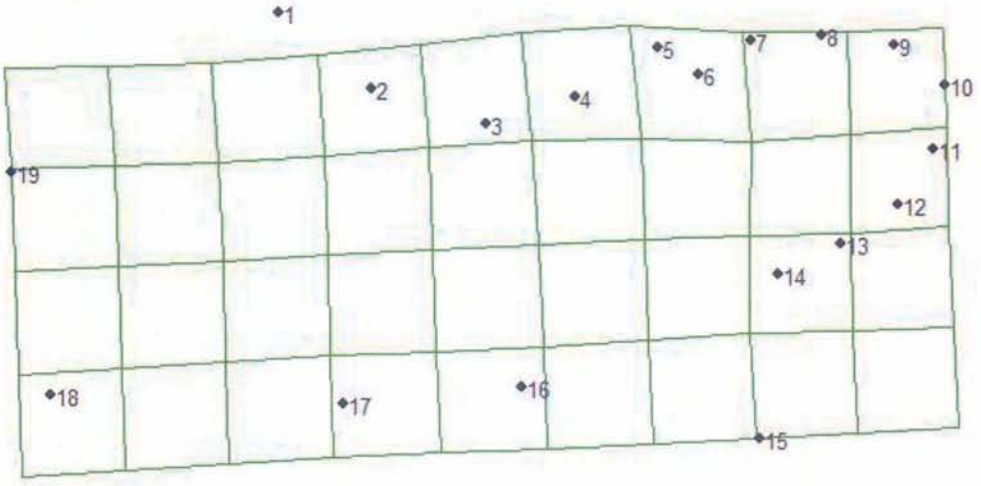

Figure 6.6: Consensus thin-plate spline (in vector mode) demonstrating the differences between black females and black males, EPI perspective.

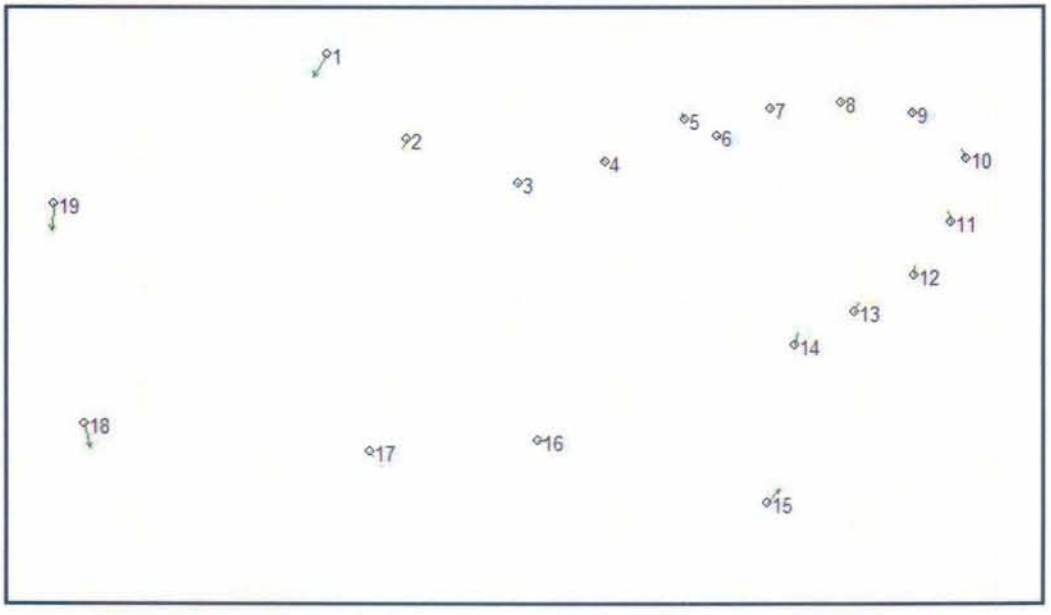

Figure 6.7: Consensus thin-plate spline in deformation mode demonstrating the differences between the reference shape (white females) and white males, EPI perspective.

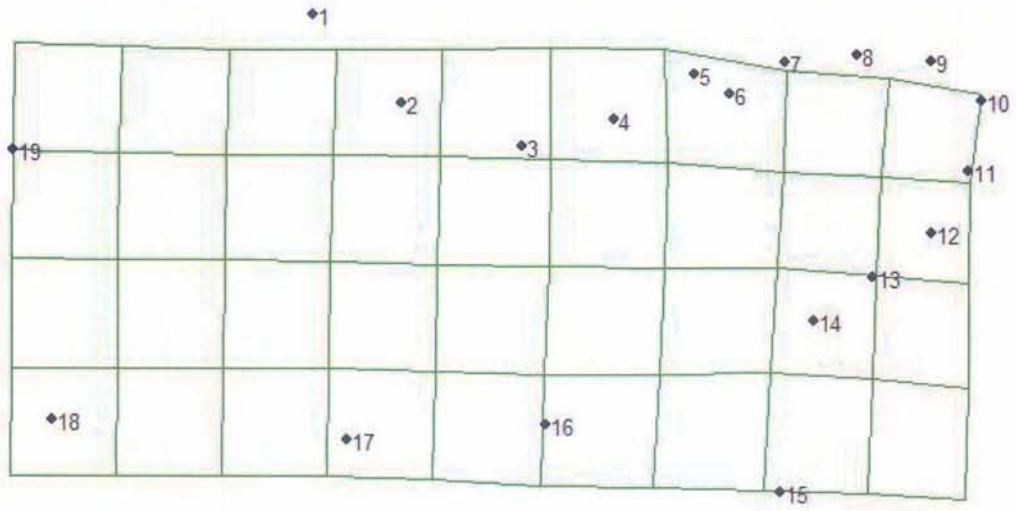

Figure 6.8: Consensus thin-plate spline (in vector mode) demonstrating the differences between white females and white males, EPI perspective.

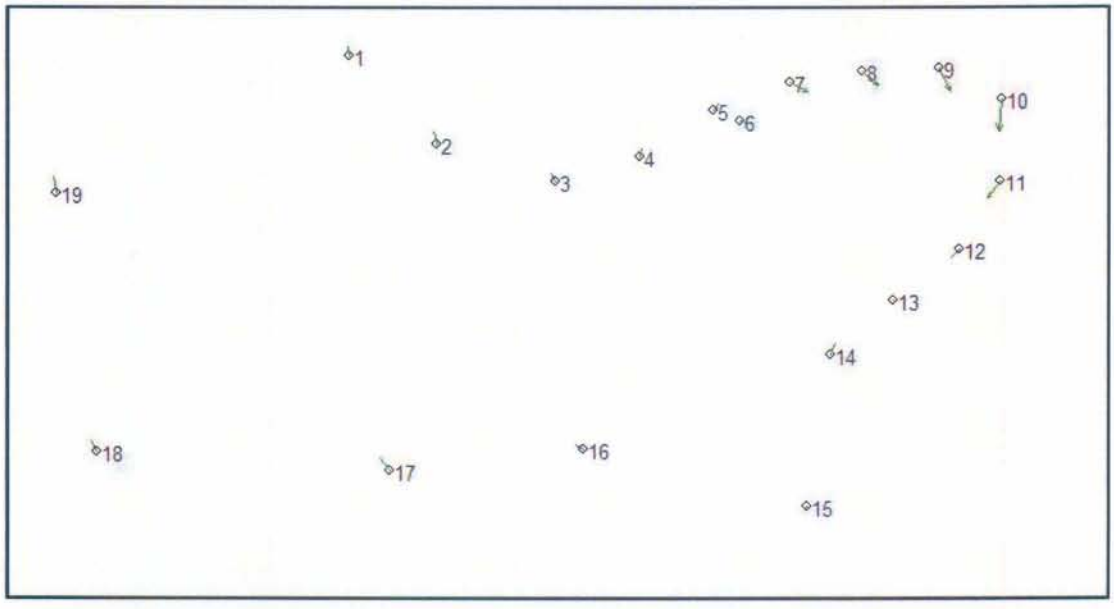

Figure 6.9: Relative warp consensus for eight groups of males and females, EPI perspective.

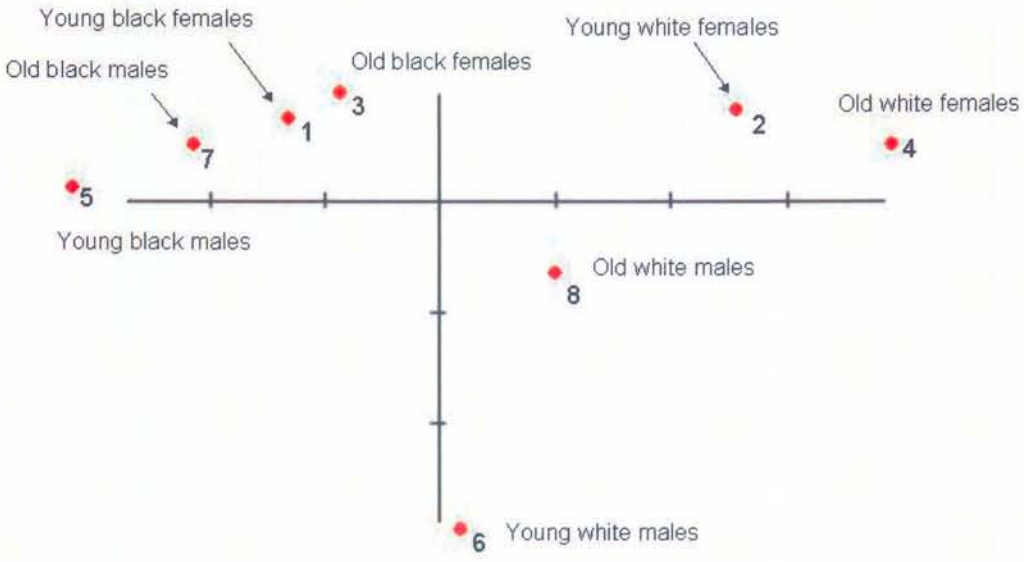

Figure 6.10: Consensus thin-plate spline (in vector mode) demonstrating the differences between young black females and old black females, EPI perspective.

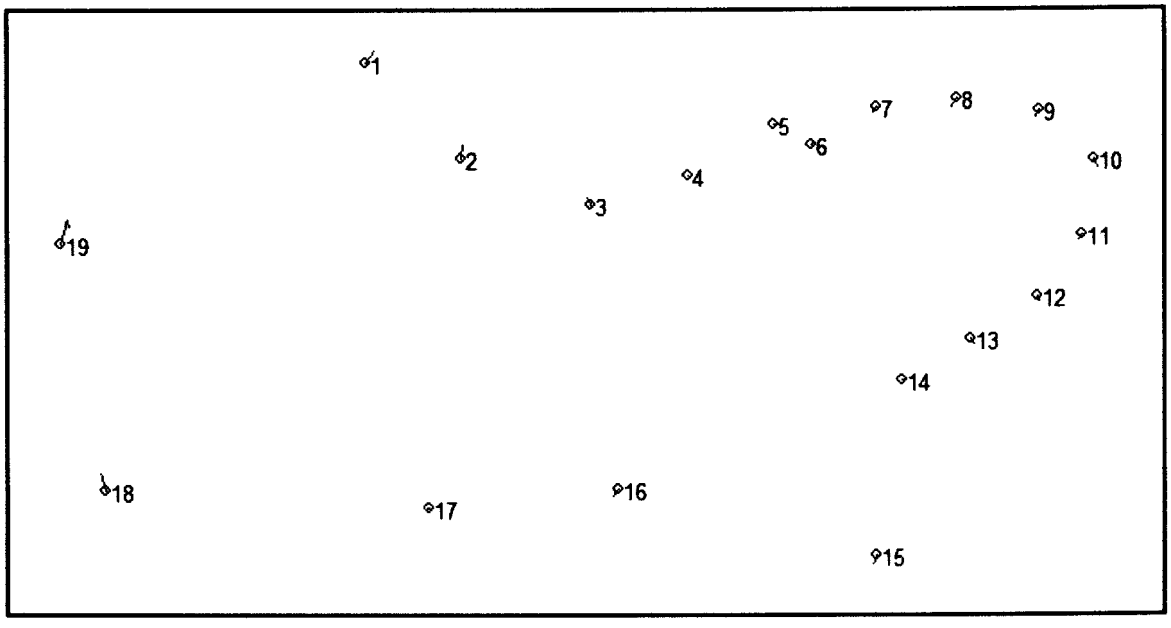

Figure 6.11: Consensus thin-plate spline (in vector mode) demonstrating the differences between young black males and old black males, EPI perspective.

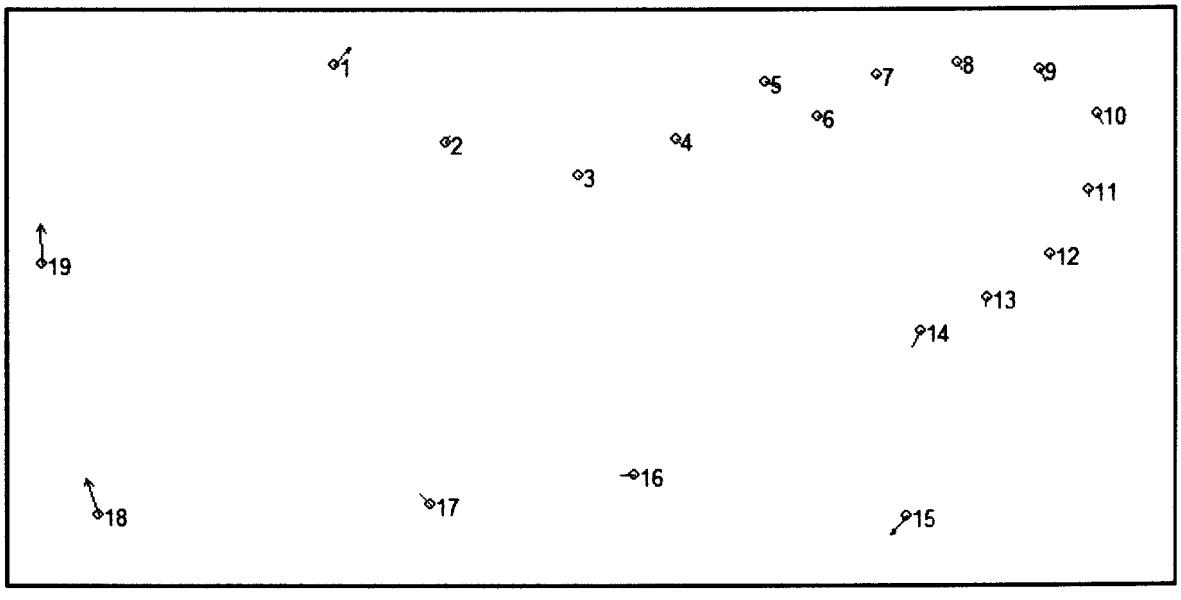

Figure 6.12: Consensus thin-plate spline (in vector mode) demonstrating the differences between young white females and old white females, EPI perspective.

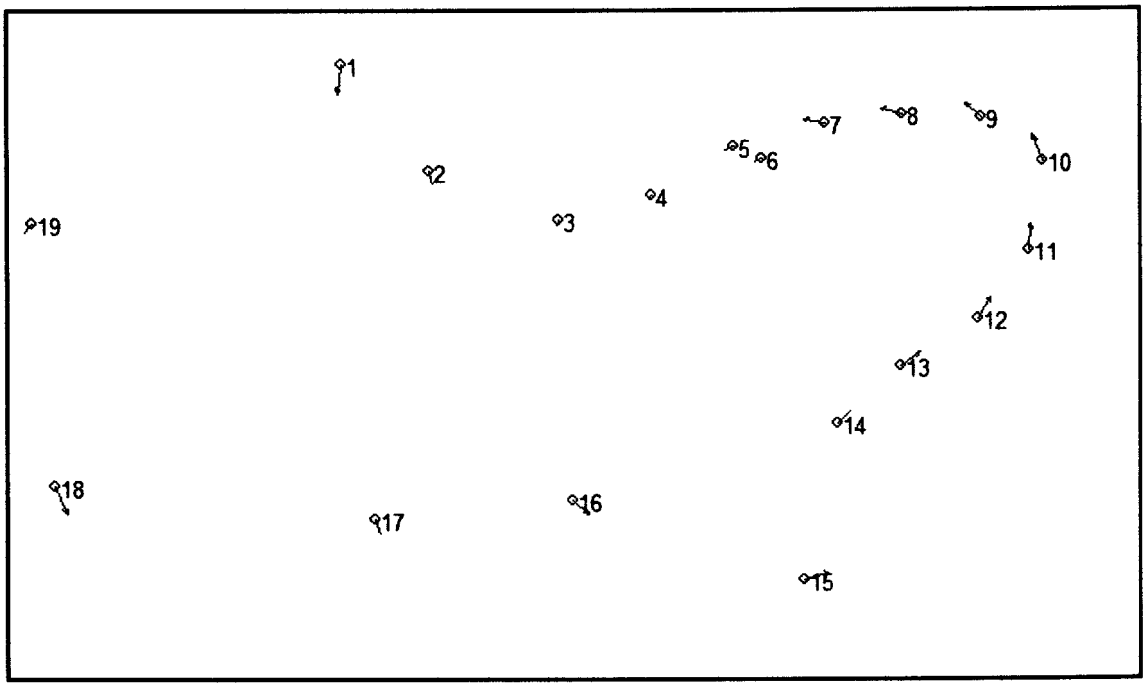

Figure 6.13: Consensus thin-plate spline (in vector mode) demonstrating the differences between young white males and old white males, EPI perspective.

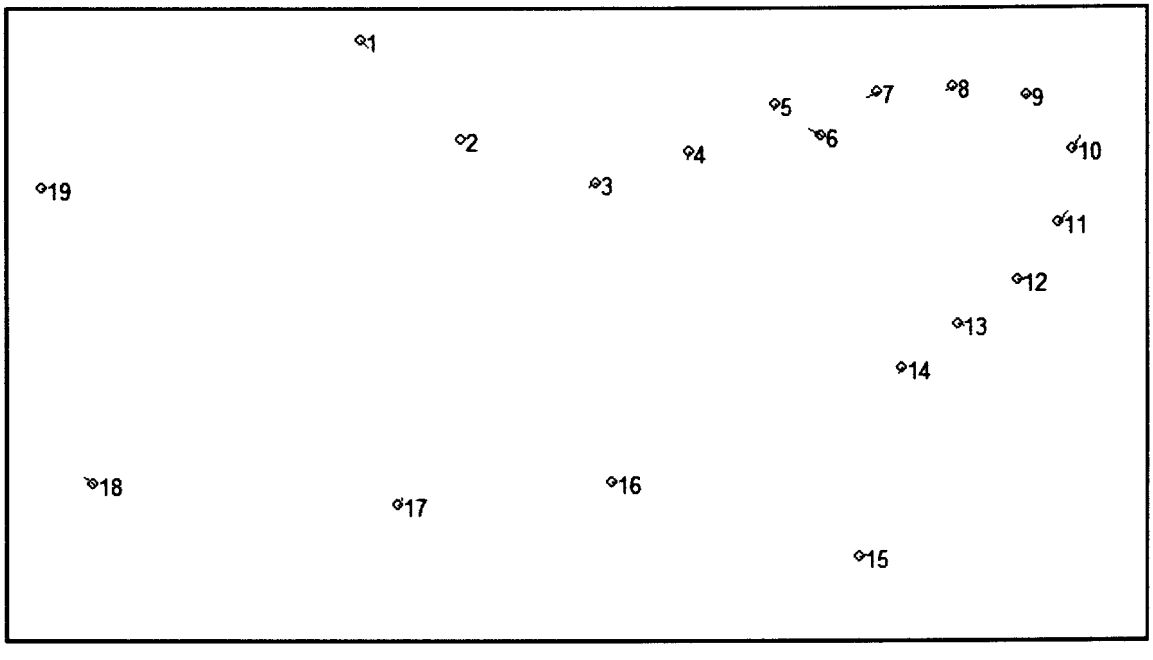

Figure 6.14: Consensus relative warp analysis of females and males, OL perspective.

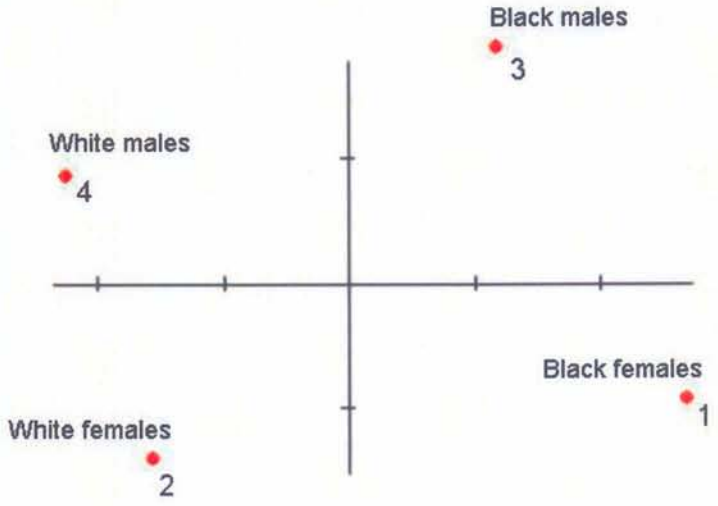

Figure 6.15: Consensus thin-plate spline reference shape of all females and all males from the OL perspective.

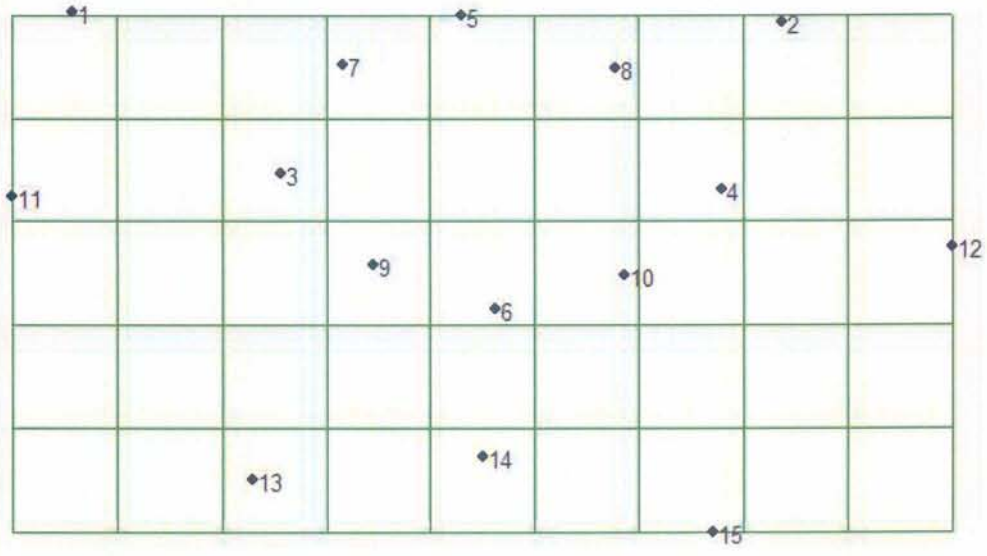

Figure 6.16: Consensus thin-plate spline in deformation mode demonstrating the differences between the reference shape (all females) and all males, OL perspective.

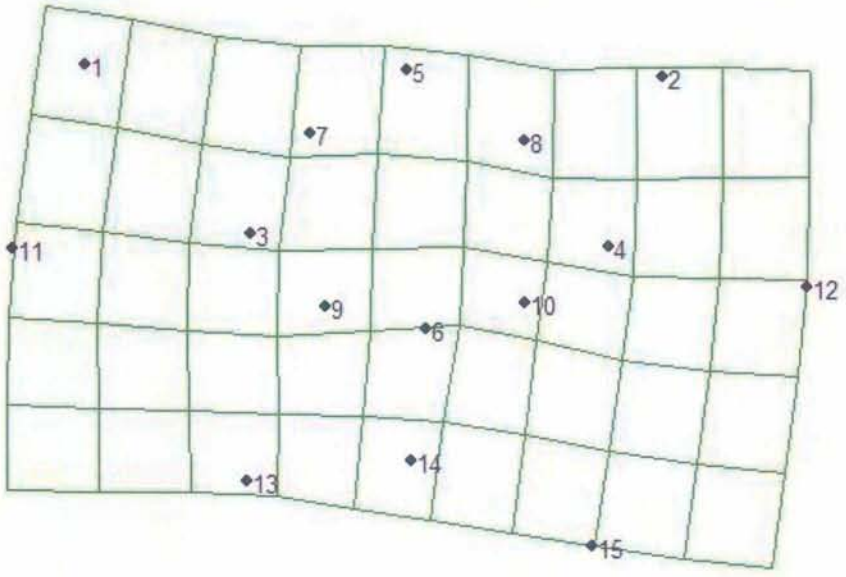

Figure 6.17: Consensus thin-plate spline (in vector mode) demonstrating the differences between all females and all males, OL perspective.

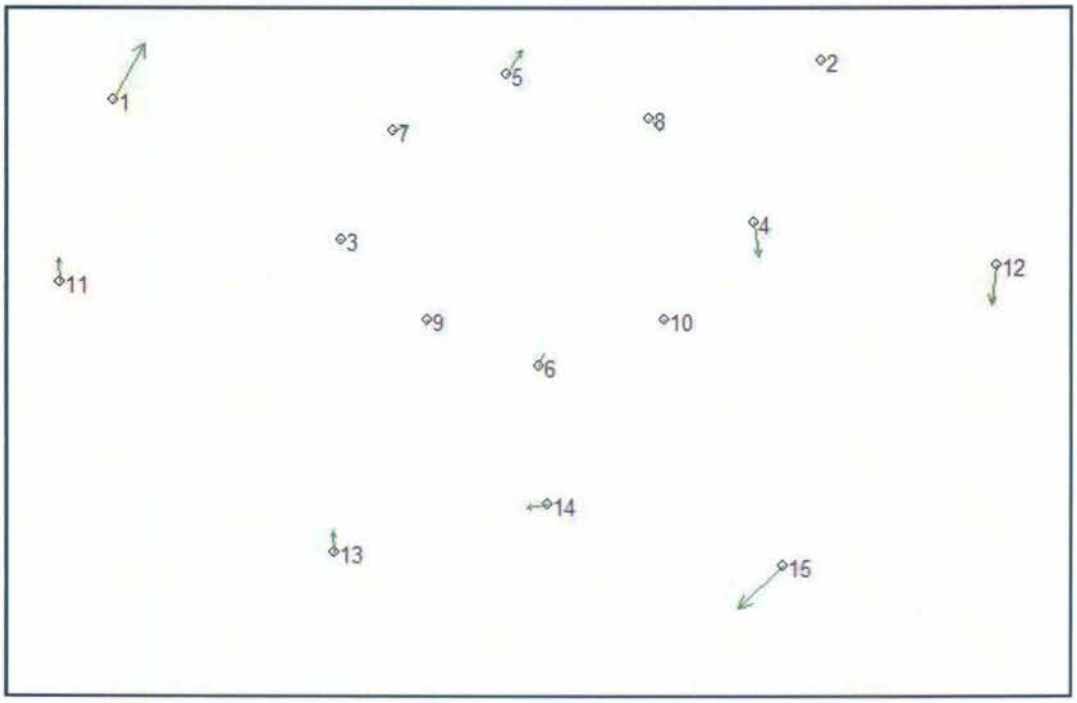

Figure 6.18: Consensus thin-plate spline in deformation mode demonstrating the differences between the reference shape (black females) and black males, OL perspective.

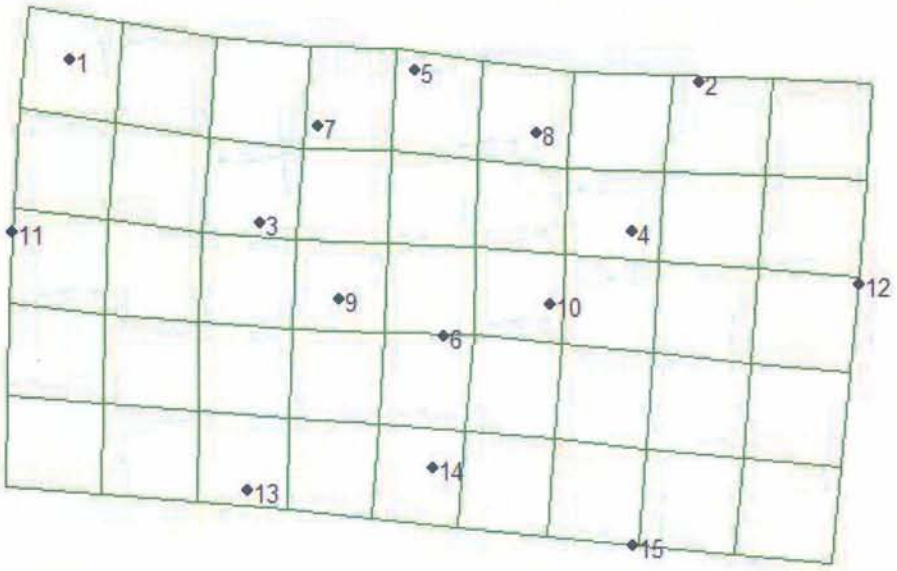

Figure 6.19: Consensus thin-plate spline (in vector mode) demonstrating the differences between black females and black males, OL perspective.

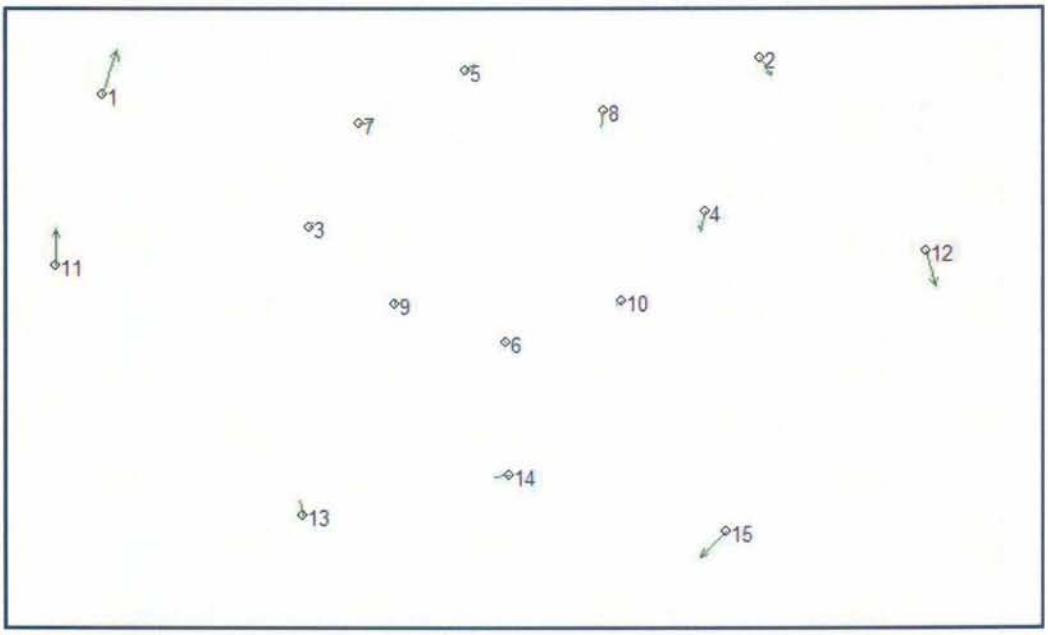

Figure 6.20: Consensus thin-plate spline in deformation mode demonstrating the differences between the reference shape (white females) and white males, OL perspective.

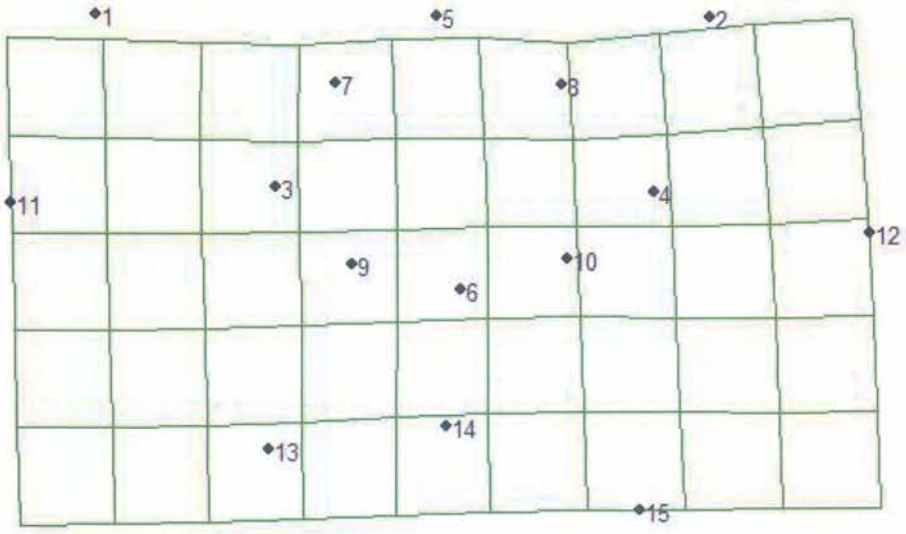

Figure 6.21: Consensus thin-plate spline (in vector mode) demonstrating the differences between white females and white males, OL perspective.

Figure 6.22: Relative warp consensus for eight groups of males and females, OL perspective.

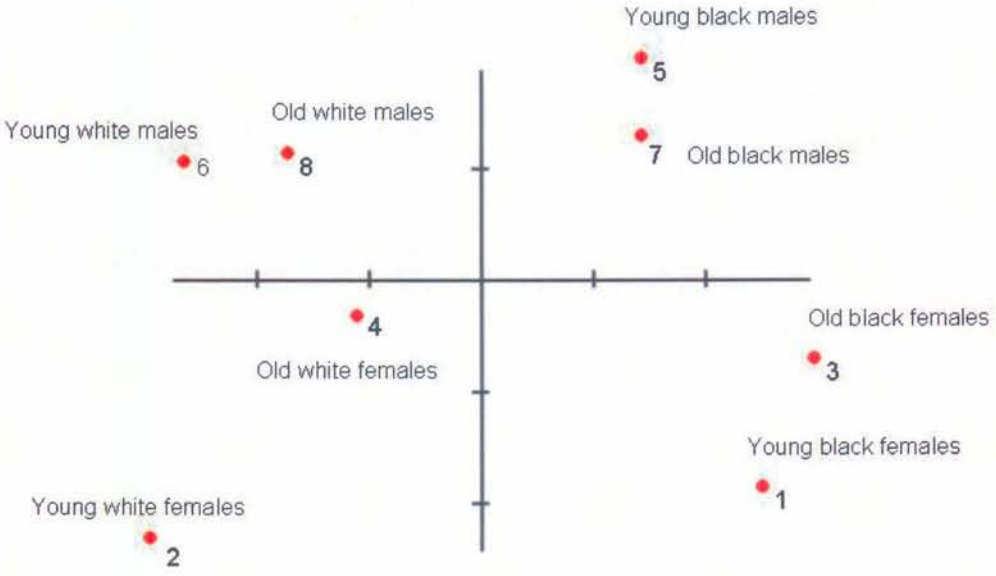

Figure 6.23: Consensus thin-plate spline (in vector mode) demonstrating the differences between young black females and old black females, OL perspective.

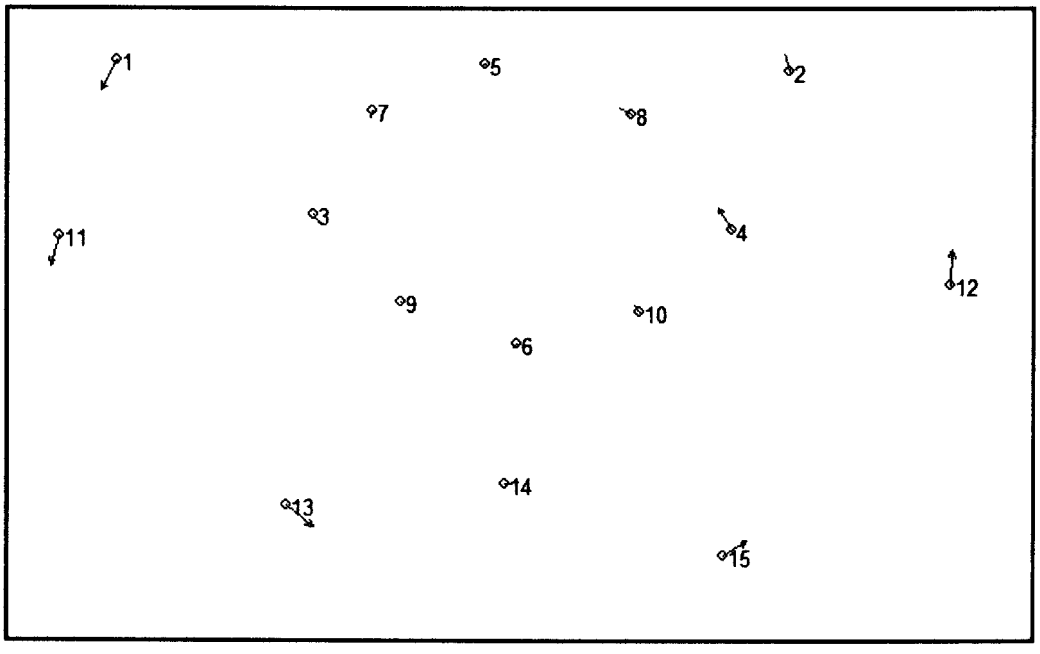

Figure 6.24: Consensus thin-plate spline (in vector mode) demonstrating the differences between young black males and old black males, OL perspective.

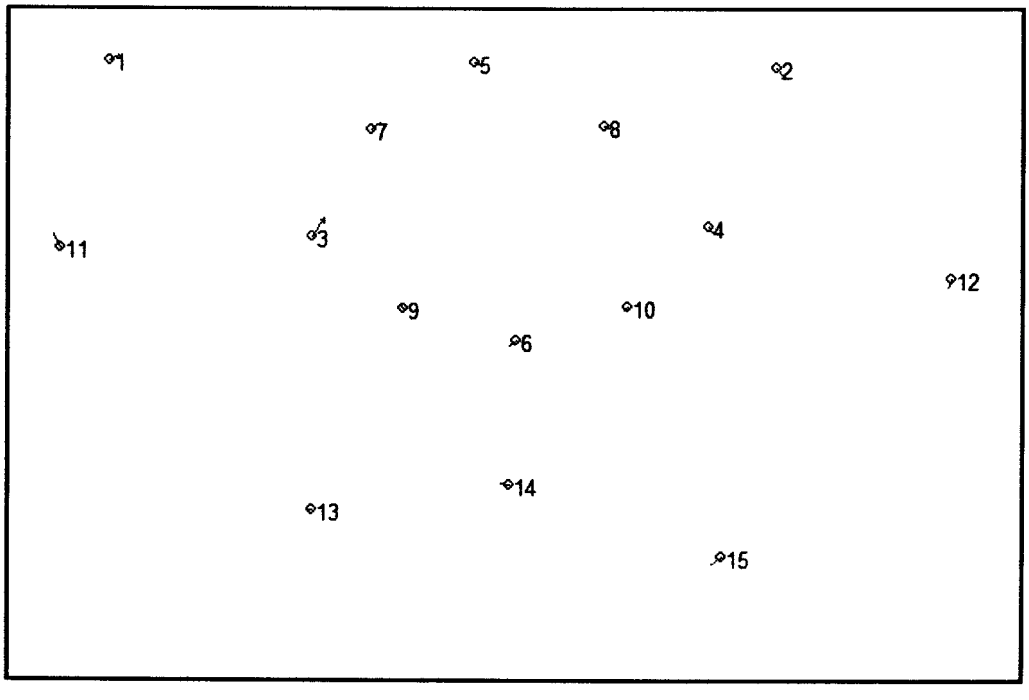

6.25: Consensus thin-plate spline (in vector mode) demonstrating the differences between young white females and old white females, OL perspective.

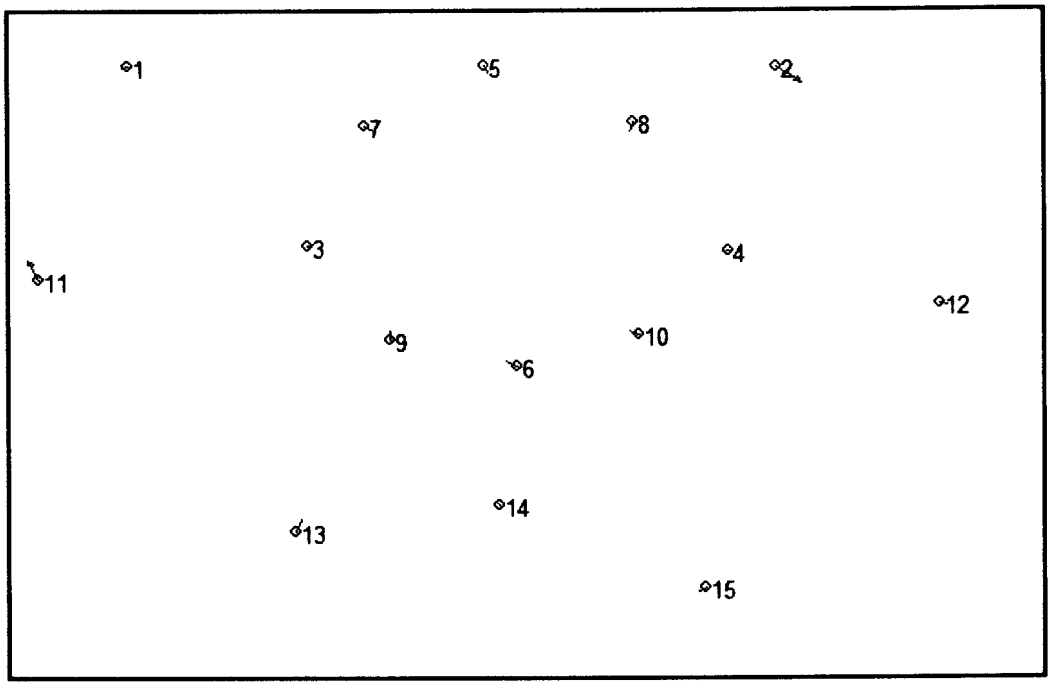

Figure 6.26: Consensus thin-plate spline (in vector mode) demonstrating the differences between young white males and old white males, OL perspective.

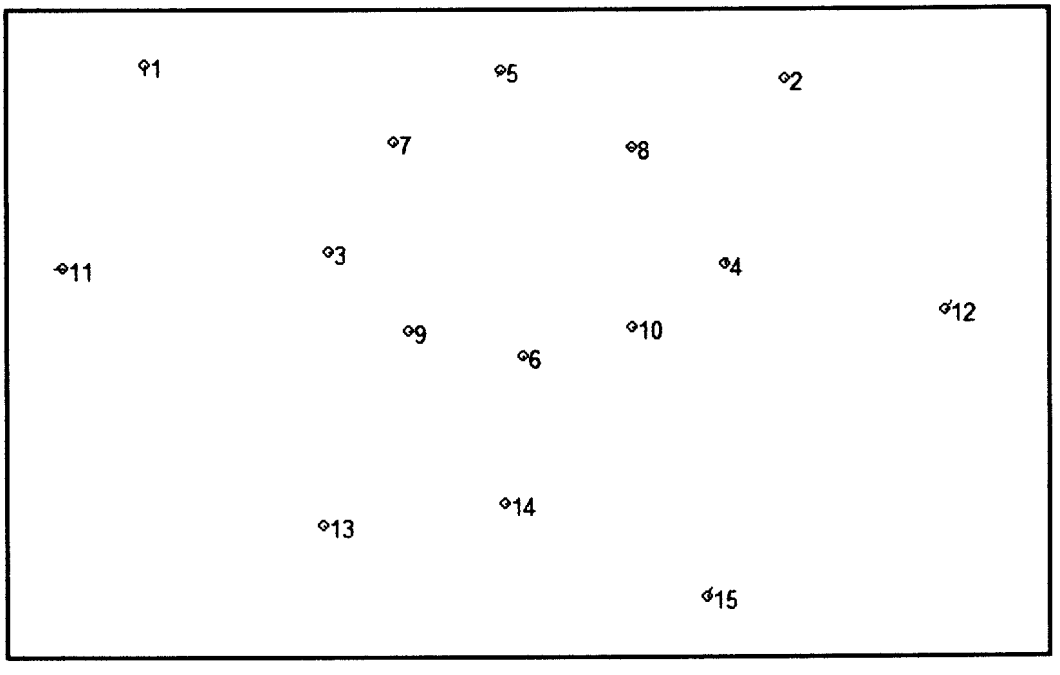

Figure 6.27: Consensus relative warp analysis of females and males, SUB perspective.

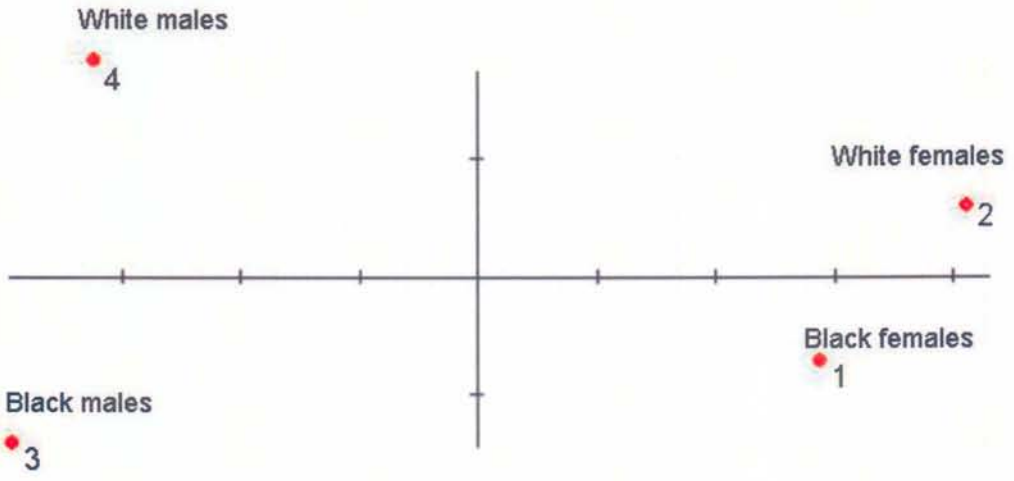

Figure 6.28: Consensus thin-plate spline reference shape of all females and all males from the SUB perspective.

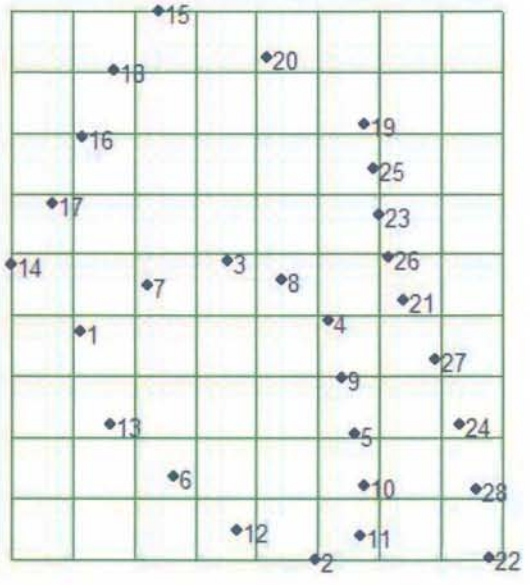

Figure 6.29: Consensus thin-plate spline in deformation mode demonstrating the differences between the reference shape (all females) and all males, SUB perspective.

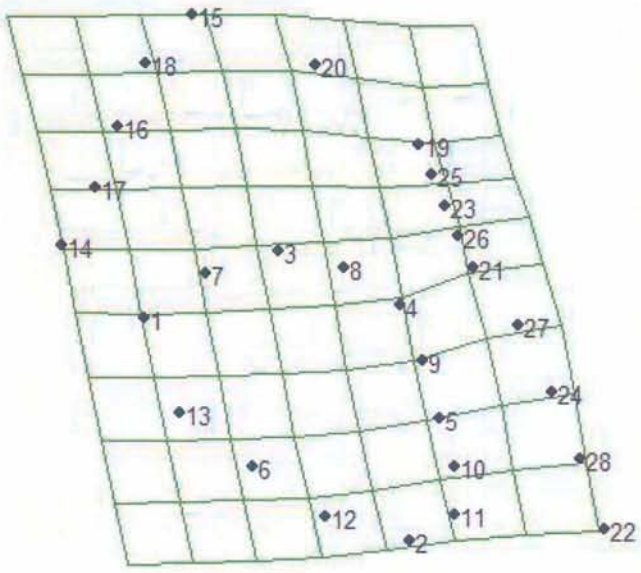

Figure 6.30: Consensus thin-plate spline (in vector mode) demonstrating the differences between all females and all males, SUB perspective.

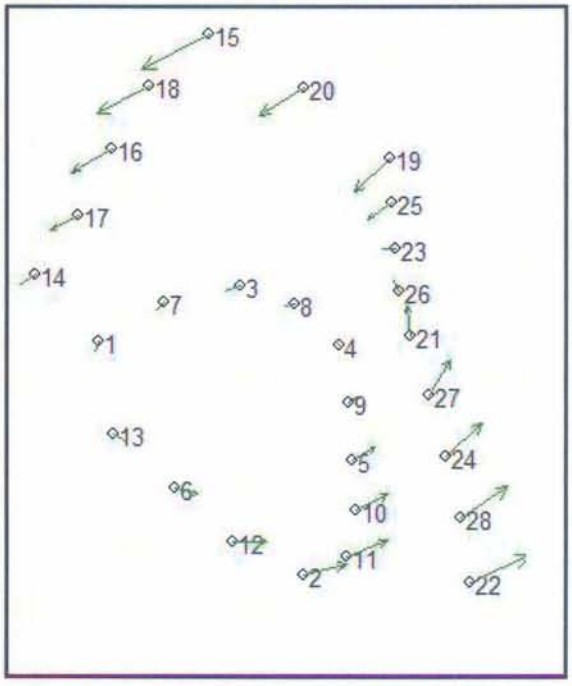

Figure 6.31: Consensus thin-plate spline in deformation mode demonstrating the differences between the reference shape (black females) and black males, SUB perspective.

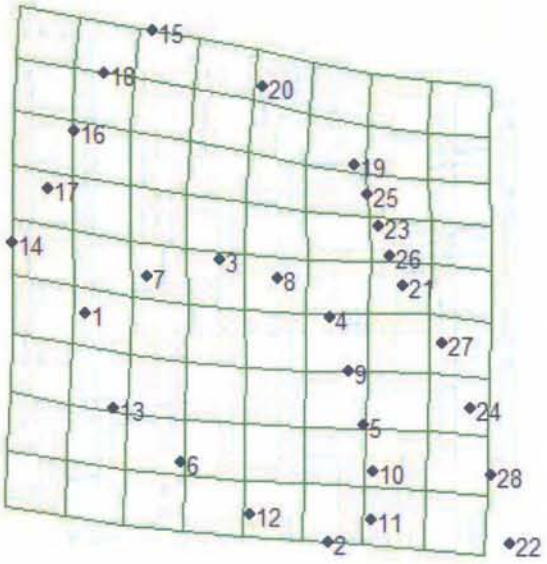

Figure 6.32: Consensus thin-plate spline (in vector mode) demonstrating the differences between black females and black males, SUB perspective.

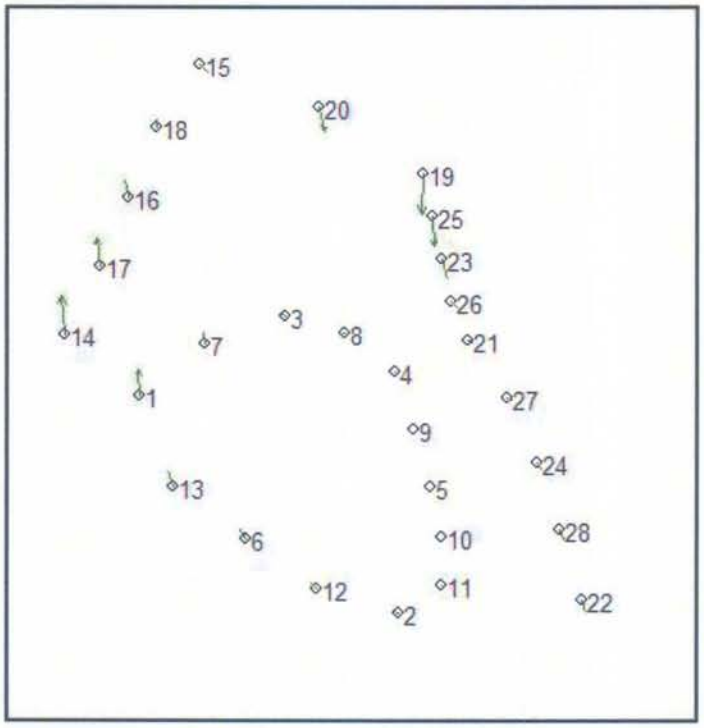

Figure 6.33: Consensus thin-plate spline in deformation mode demonstrating the differences between the reference shape (white females) and white males, SUB perspective.

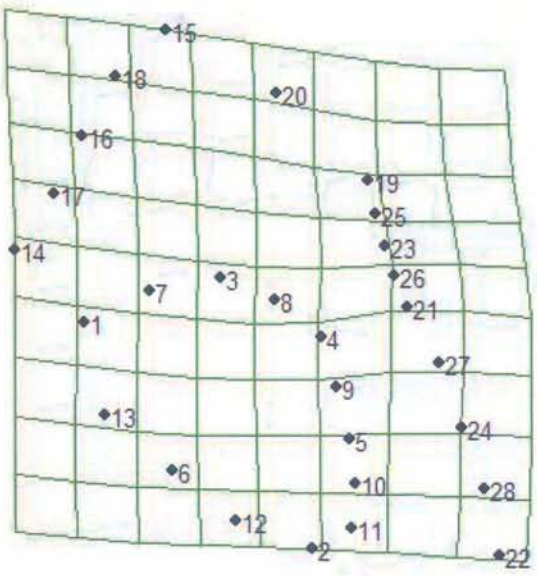

Figure 6.34: Consensus thin-plate spline (in vector mode) demonstrating the differences between white females and white males, SUB perspective.

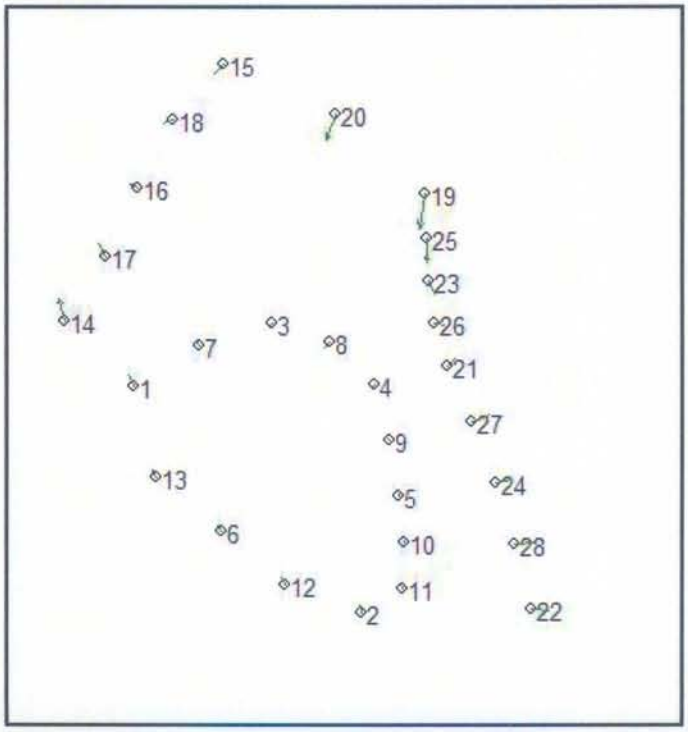

Figure 6.35: Relative warp consensus for eight groups of males and females, SUB perspective.

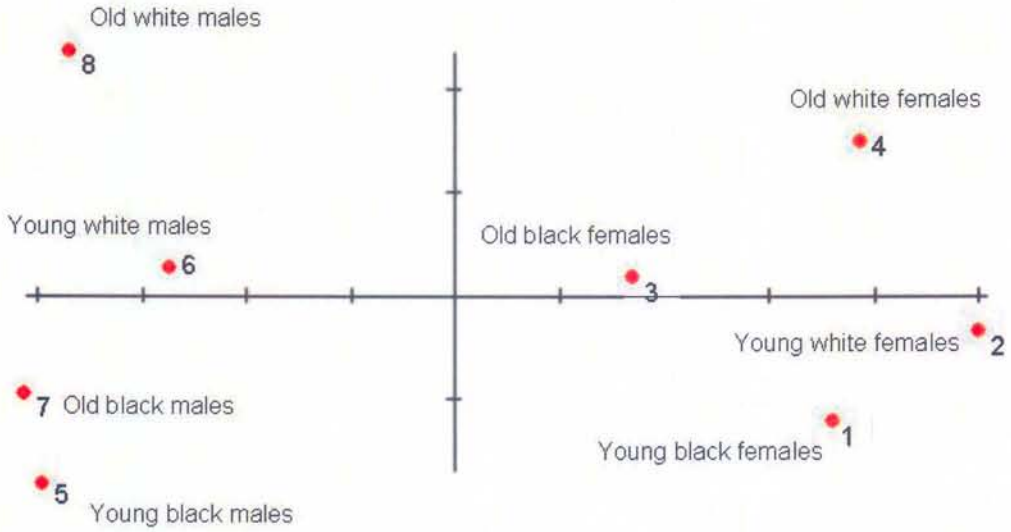

Figure 6.36: Consensus thin-plate spline (in vector mode) demonstrating the differences between young black females and old black females, SUB perspective.

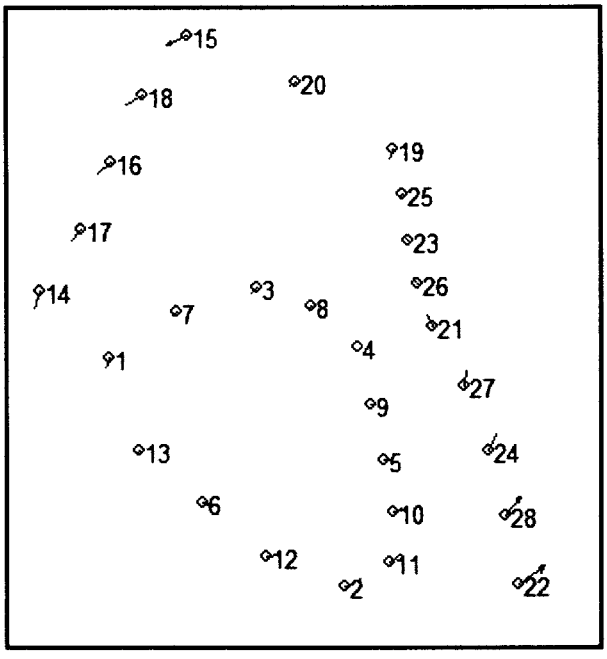

Figure 6.37: Consensus thin-plate spline (in vector mode) demonstrating the differences between young black males and old black males, SUB perspective.

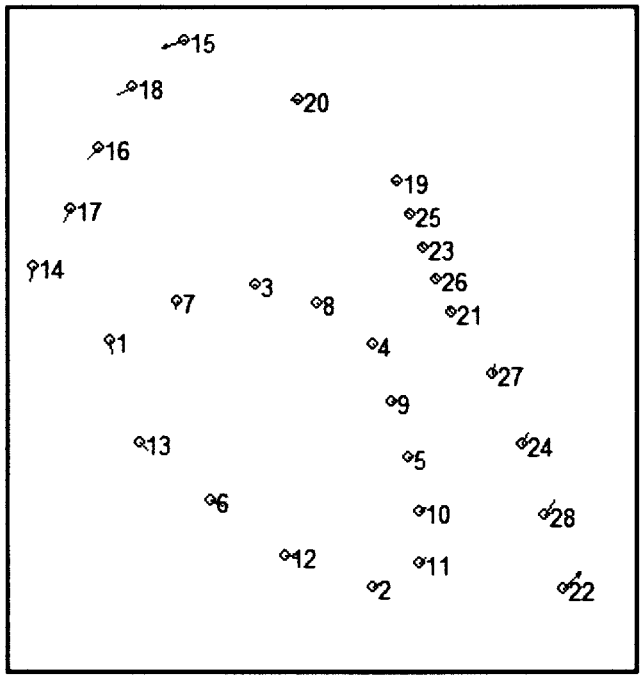

Figure 6.38: Consensus thin-plate spline (in vector mode) demonstrating the differences between young white females and old white females, SUB perspective.

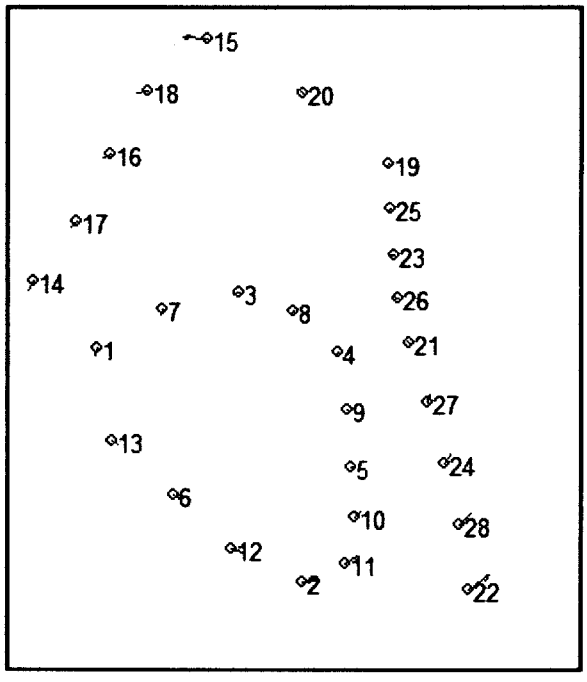

Figure 6.39: Consensus thin-plate spline (in vector mode) demonstrating the differences between young white males and old white males, SUB perspective.

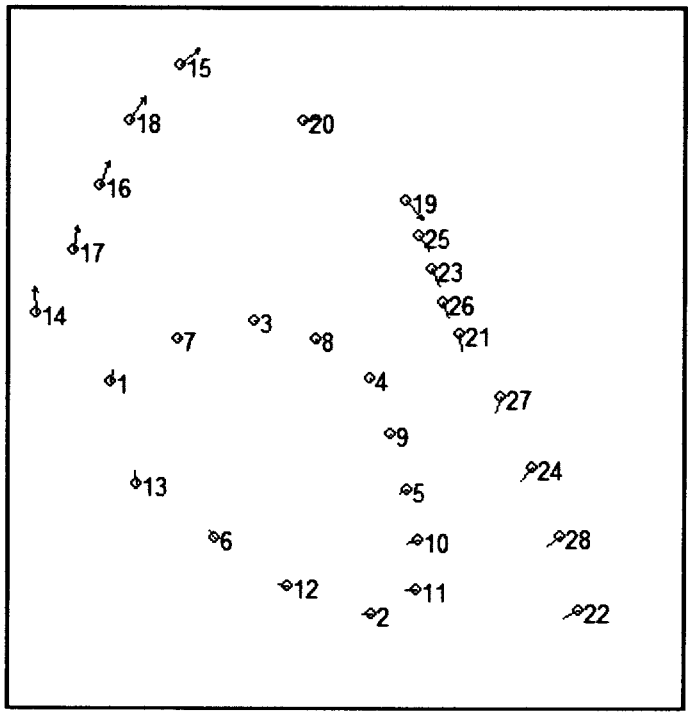

Figure 6.40: Consensus relative warp analysis of females and males, SCI perspective.

Figure 6.41: Consensus thin-plate spline reference shape of all females and all males from the SCI perspective.

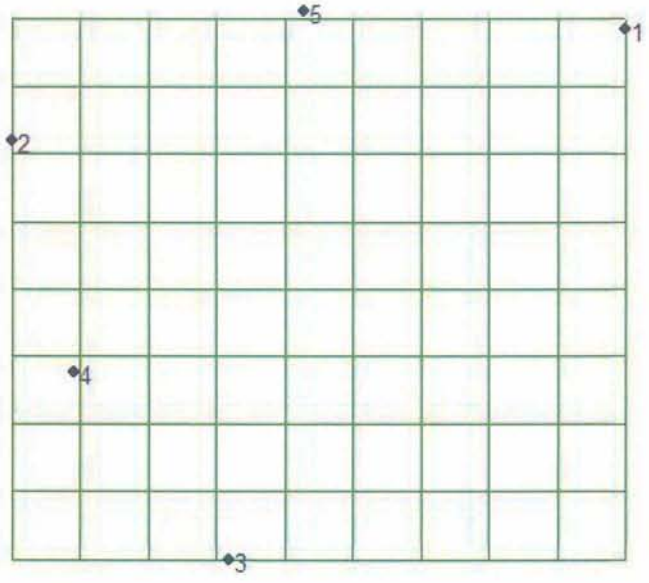

Figure 6.42: Consensus thin-plate spline in deformation mode demonstrating the differences between the reference shape (all females) and all males, SCI perspective.

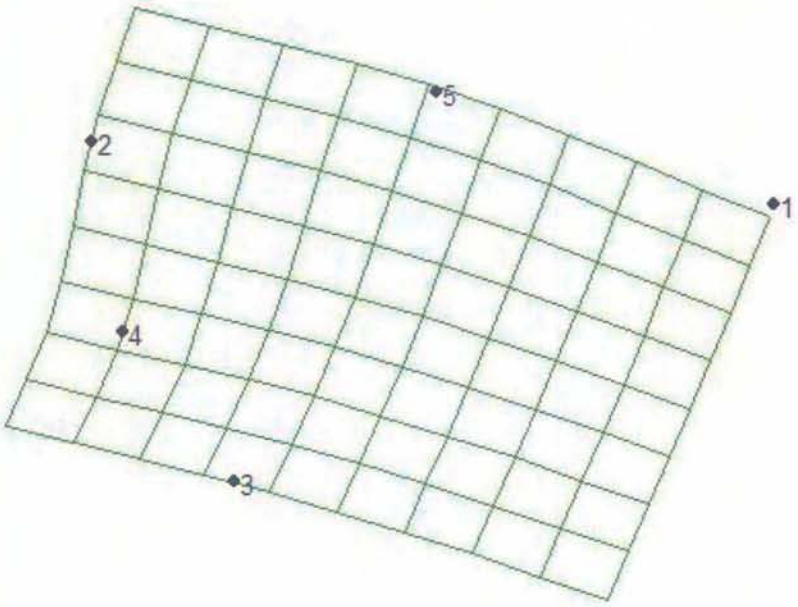

Figure 6.43: Consensus thin-plate spline (in vector mode) demonstrating the differences between all females and all males, SCI perspective.

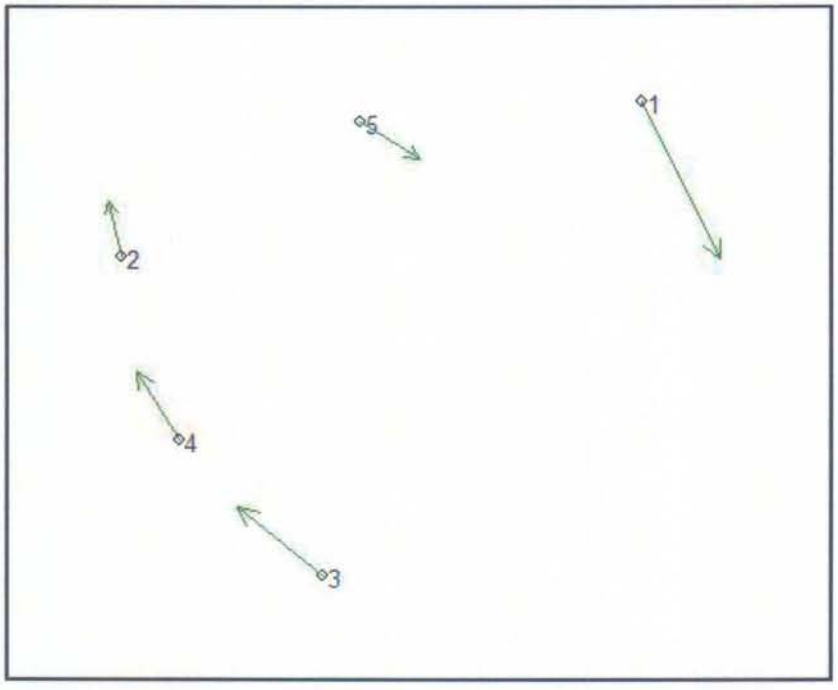

Figure 6.44: Consensus thin-plate spline in deformation mode demonstrating the differences between the reference shape (black females) and black males, SCI perspective.

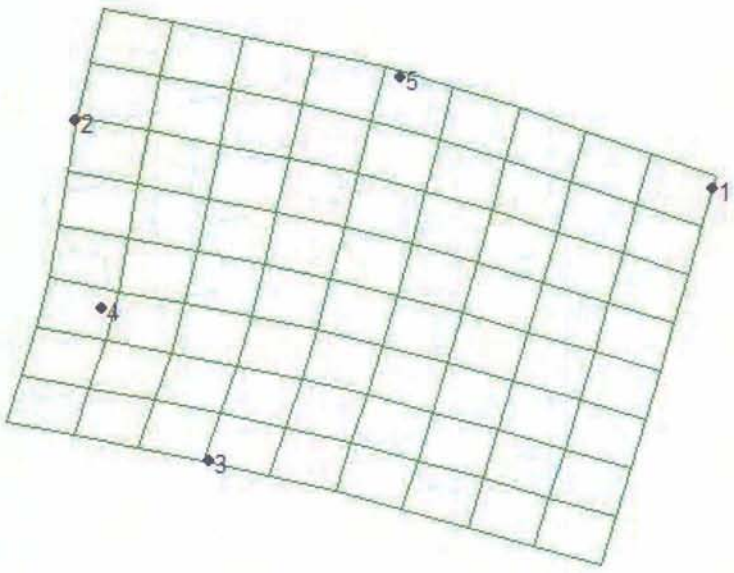

Figure 6.45: Consensus thin-plate spline (in vector mode) demonstrating the differences between black females and black males, SCI perspective.

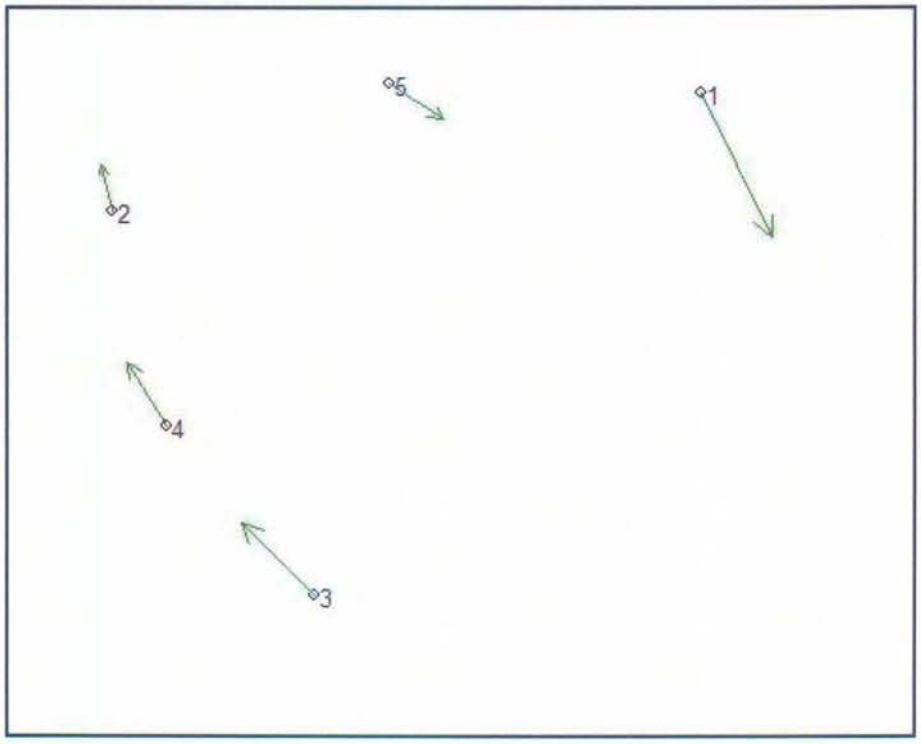

Figure 6.46: Consensus thin-plate spline in deformation mode demonstrating the differences between the reference shape (white females) and white males, SCI perspective.

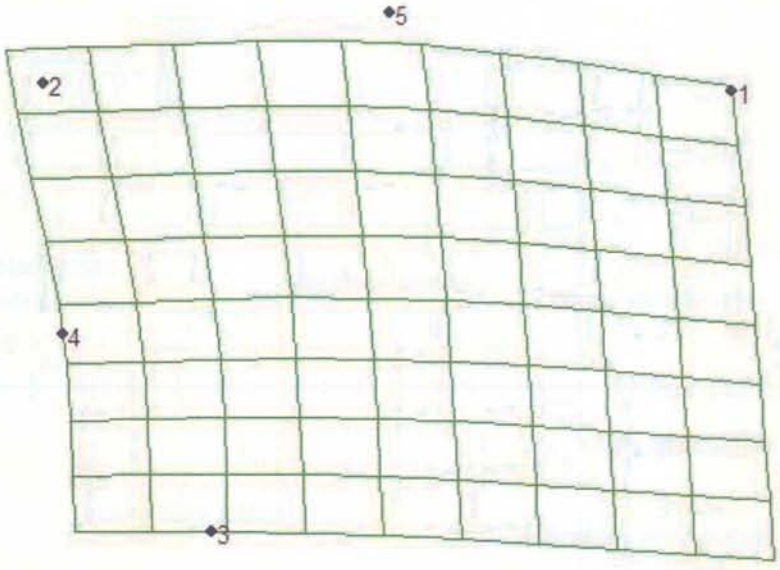

Figure 6.47: Consensus thin-plate spline (in vector mode) demonstrating the differences between white females and white males, SCI perspective.

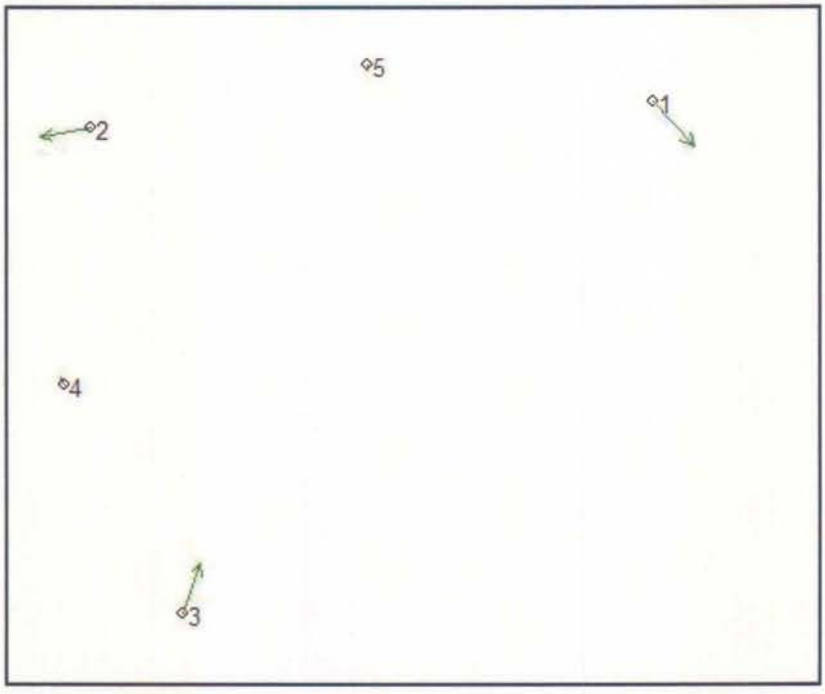

Figure 6.48: Relative warp consensus for eight groups of males and females, SCI perspective.

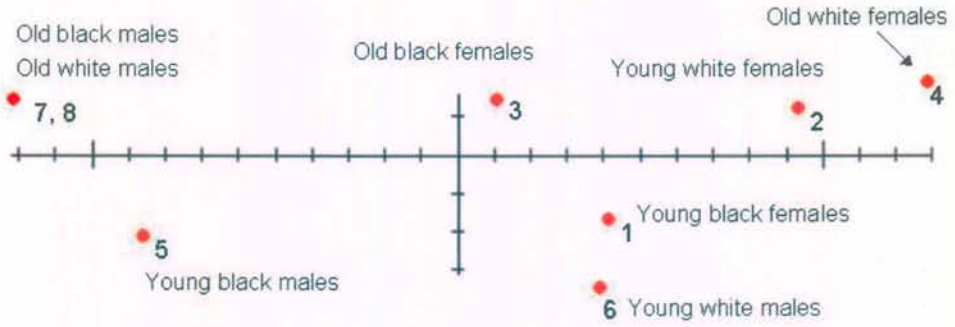

Figure 6.49: Consensus thin-plate spline (in vector mode) demonstrating the differences between young black females and old black females, SCI perspective.

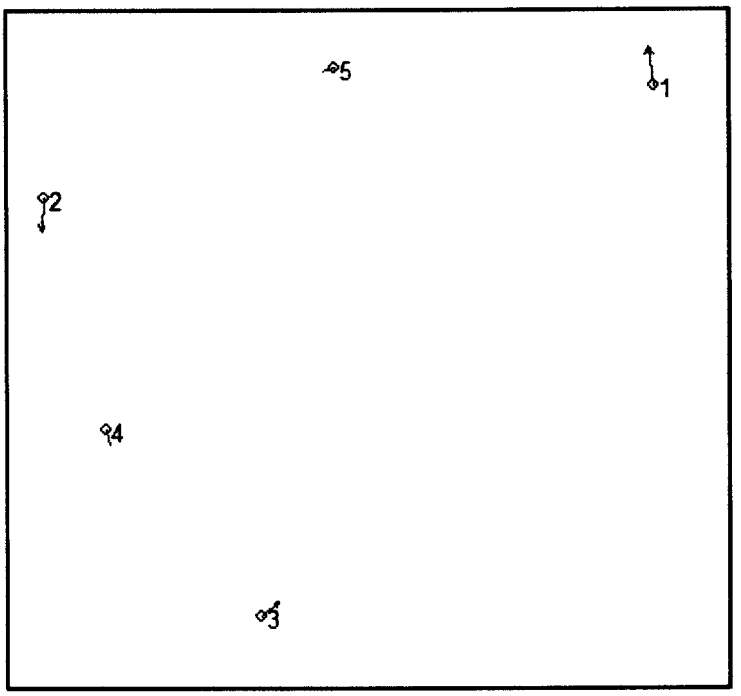

Figure 6.50: Consensus thin-plate spline (in vector mode) demonstrating the differences between young black males and old black males, SCI perspective.

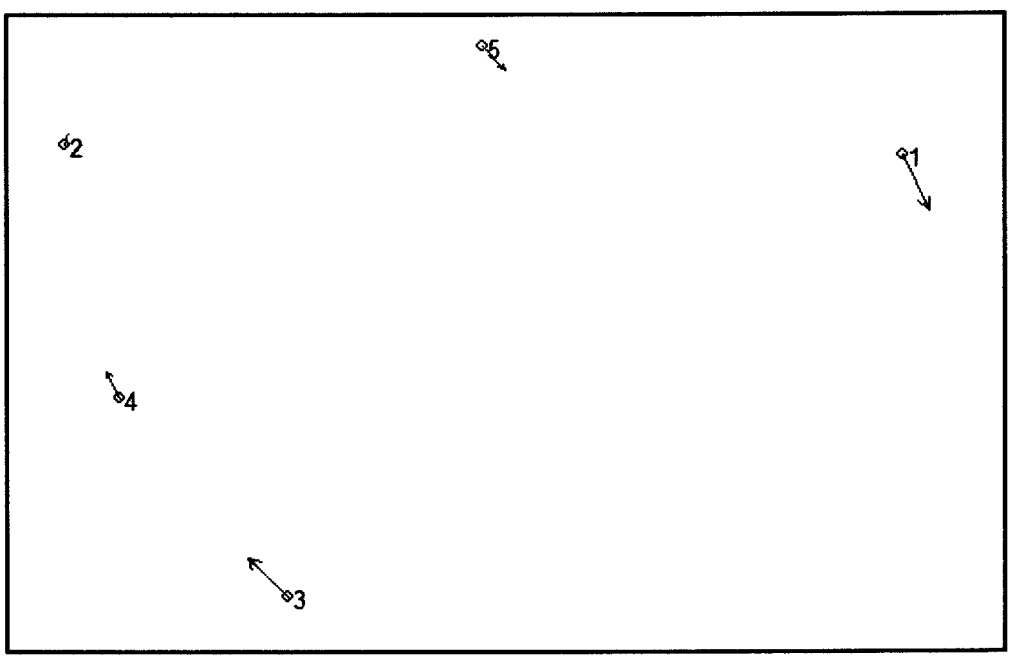

6.51: Consensus thin-plate spline (in vector mode) demonstrating the differences between young white females and old white females, SCI perspective.

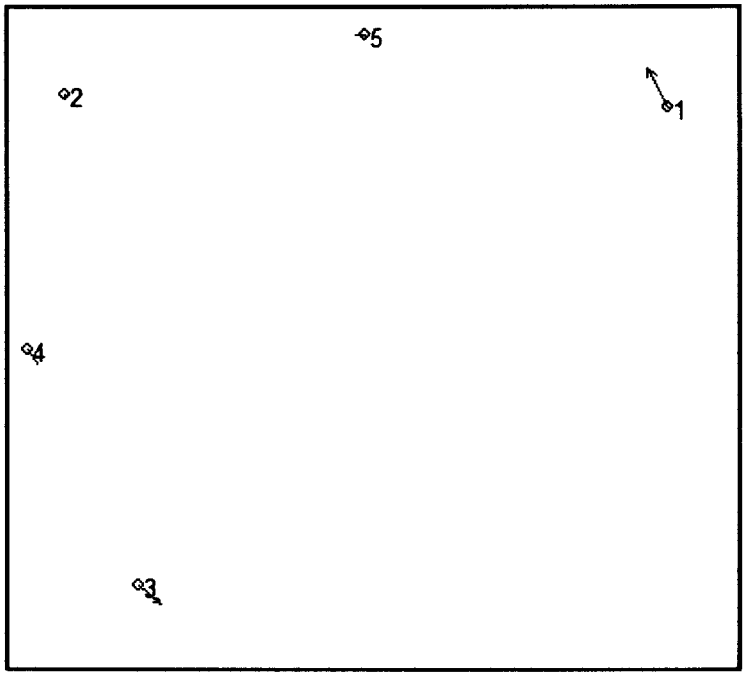

Figure 6.52: Consensus thin-plate spline (in vector mode) demonstrating the differences between young white males and old white males, SCI perspective.